Characterization of the GPI-anchored lipid transfer proteins in the moss Physcomitrella patens

Edstam, Monika M.; Laurila, Maiju; Höglund, Andrey; Raman, Amitha; Dahlström, Käthe; Salminen, Tiina; Edqvist, Johan; Blomqvist, Kristina

Published in:
Plant Physiology and Biochemistry

DOI:
10.1016/j.plaphy.2013.12.001

Published: 01/01/2014

Plant Physiology and Biochemistry 75 (2014) 55–69

Contents lists available at ScienceDirect

Plant Physiology and Biochemistry

journal homepage: www.elsevier.com/locate/plaphy

Research article

Characterization of the GPI-anchored lipid transfer proteins in the moss *Physcomitrella patens*

Monika M. Edstam [a], Maiju Laurila [b], Andrey Höglund [a], Amitha Raman [a], Käthe M. Dahlström [b], Tiina A. Salminen [b], Johan Edqvist [a,*], Kristina Blomqvist [a]

[a] IFM, Linköping University, 581 83 Linköping, Sweden
[b] Structural Bioinformatics Laboratory, Department of Biosciences, Åbo Akademi University, FI-20520 Turku, Finland

ARTICLE INFO

Article history:
Received 7 November 2013
Accepted 2 December 2013
Available online 17 December 2013

Keywords:
LTP
Cuticle
Moss
Lipids
Heat stability
Circular dichroism
Cutin

ABSTRACT

The non-specific lipid transfer proteins (nsLTPs) are characterized by a compact structure with a central hydrophobic cavity very suitable for binding hydrophobic ligands, such as lipids. The nsLTPs are encoded by large gene families in all land plant lineages, but seem to be absent from green algae. The nsLTPs are classified to different types based on molecular weight, sequence similarity, intron position or spacing between the cysteine residues. The Type G nsLTPs (LTPGs) have a GPI-anchor in the C-terminal region which may attach the protein to the exterior side of the plasma membrane. Here, we present the first characterization of nsLTPs from an early diverged plant, the moss *Physcomitrella patens*. Moss LTPGs were heterologously produced and purified from *Pichia pastoris*. The purified moss LTPGs were found to be extremely heat stable and showed a binding preference for unsaturated fatty acids. Structural modeling implied that high alanine content could be important for the heat stability. Lipid profiling revealed that cutin monomers, such as C_{16} and C_{18} mono- and di-hydroxylated fatty acids, could be identified in *P. patens*. Expression of a moss LTPG-YFP fusion revealed localization to the plasma membrane. The expressions of many of the moss LTPGs were found to be upregulated during drought and cold treatments.

1. Introduction

The non-specific lipid transfer proteins (nsLTPs) are only found in land plants, where they are very abundant and encoded by large gene families in both non-vascular and vascular species (Boutrot et al., 2008; Edstam et al., 2011). The first nsLTPs were found almost 40 years ago. Initially, the nsLTPs were thought to be involved in intracellular lipid trafficking, since they have the ability to transfer lipids between membranes *in vitro* (Kader, 1975). Later they were shown to be secreted to the extracellular matrix, which made a role in intracellular lipid trafficking more unlikely (Sterk et al., 1991; Thoma et al., 1994). The *in vivo* function of the nsLTPs is still unclear. However, different angles of research have opened for many different hypotheses. The more well-established theories include an involvement of nsLTPs in long distance signaling, pathogen defense, cuticle formation, suberin biosynthesis, pollen tube adhesion, seed germination and fruit ripening (Debono et al., 2009; Edqvist and Farbos, 2002; Edstam et al., 2013; Eklund and Edqvist, 2003; Maldonado et al., 2002; Park and Lord, 2003; Park et al., 2002; Tomassen et al., 2007).

The nsLTPs are small, soluble proteins, usually about 7–9 kDa in size (Kader, 1996). Their structure consists of four or five alpha helices, with a central hydrophobic cavity where the lipid binding takes place (Gincel et al., 1994; Lee et al., 1998; Pons et al., 2003; Shin et al., 1995). The nsLTPs have been shown to bind a variety of lipid substrates including phospholipids, fatty acids and acyl-coenzyme A (Guerbette et al., 1999; Smith et al., 2013; Zachowski et al., 1998). The nsLTPs are very stable to heat and denaturation agents due to four stabilizing disulphide bridges (Lindorff-Larsen and Winther, 2001; Berecz et al., 2010). The bridges are composed by eight Cys residues, conserved in a specific pattern, known as the 8CM, with the general form C-x_n-C-x_n-CC-CxC-x_n-C-x_n-C. The nsLTPs have traditionally been divided in Type 1 (LTP1) and Type 2 (LTP2). These types differ by their molecular size, where LTP1 has a size of about 90 amino acids, while LTP2 has about 70 amino acids. LTP1 and LTP2 can also be distinguished by their 3D-structure due to a different pairing of the disulfide bridges (Douliez et al., 2001; Pons et al., 2003). The central residue between Cys5 and Cys6 of the 8CM may govern the Cys-pairing and influence the overall fold of the protein (Samuel et al., 2002). For instance, in rice

* Corresponding author. Tel.: +46 (0)13 281288; fax: +46 (0)13 13 75 68.
E-mail address: Johan.Edqvist@liu.se (J. Edqvist).

0981-9428/$ – see front matter © 2013 Elsevier Masson SAS. All rights reserved.
http://dx.doi.org/10.1016/j.plaphy.2013.12.001

(*Oryza sativa*) LTP1 a hydrophilic Asn present between Cys5 and Cys6 is projected to the surface of the protein. This results in the pairing of Cys1 with Cys6 and Cys5 with Cys8. On the other hand, in rice LTP2 a hydrophobic Phe between Cys5 and Cys6 is buried inside, changing the pairing of Cys1 to Cys5 and of Cys6 to Cys8. The fold also influences the structure of the hydrophobic cavity, which is a tunnel in LTP1 and a triangular hollow box in LTP2 (Pons et al., 2003; Samuel et al., 2002). These structural differences might have an impact on the function or biological role of the different types of nsLTPs. More recently other nsLTPs that are not readily classified into either LTP1 or LTP2 have been identified. One example is the DIR1 nsLTP from *Arabidopsis thaliana*, which has a 3D-folding that is clearly different from both LTP1 and LTP2, although it has a similar pairing of the disulfide bridges as LTP2 (Lascombe et al., 2008).

We have shown that the nsLTPs in early diverging plants, such as mosses and liverworts, could not be classified into LTP1 or LTP2. To come around this problem, we introduced a modified and expanded nsLTP-classification system that also accounts for the spacing between Cys residues, the position of a conserved intron and the post-translational addition of a glycosylphosphatidylinositol (GPI)-anchor (Edstam et al., 2011). According to this novel classification system, DIR1 belongs to Type D. Further, the 14 identified nsLTPs from the liverwort *Marchantia polymorpha* were classified into Type D or Type G, whereas the 40 identified nsLTPs from the moss *Physcomitrella patens* were grouped to Type D, Type G, Type J and Type K. Type D and Type G are found in all investigated land plants and therefore represents the earliest nsLTPs (Edstam et al., 2011).

The difference between Type D and Type G is that the genes belonging to Type G encode a C-terminal signal sequence, which leads to a posttranslational modification where a GPI-anchor is added to the protein (Ikezawa, 2002). The GPI-anchor has the ability to attach proteins to the extracellular side of the plasma membrane, from where the proteins can be released by phospholipases or taken into the cell via endocytosis (Lakhan et al., 2009; Müller et al., 2012). Type G is one of the larger nsLTP types, with 34 members in *A. thaliana* and 10 in *P. patens* (Edstam et al., 2011). There are several reports that associate lowered expression of Type G nsLTPs (LTPGs) in *A. thaliana* with reduced levels of cuticular wax or wax components (Debono et al., 2009; Lee et al., 2009; Kim et al., 2012). Furthermore, results from a coexpression analysis in *A. thaliana* and rice indicate that LTPGs are involved in the synthesis of suberin and sporopollenin (Edstam et al., 2013). In this study, we present the first characterization of nsLTPs from a non-seed plant, by investigating the properties of several LTPGs from the moss *P. patens*. In addition to this, the lipid composition of the *P. patens* cuticle was determined. We chose to characterize the LTPGs from moss due to our interest in the function and evolution of these enigmatic proteins. We show that many features found in nsLTPs from flowering plants were established already in moss.

2. Material and methods

2.1. Plant material and growth conditions

P. patens ssp. *patens* (strain Gransden 2004) was grown on BCD medium supplemented with 1 mM $CaCl_2$, 5 mM ammonium tartrate and 0.8% agar, at 25 °C under continuous light (6000 lux) (Nishiyama et al., 2000) in a tissue culture chamber (CU-36L/5, Percival, Perry, Iowa, USA). For liquid cultures the agar was omitted.

2.2. Sequence analysis

Multiple sequence alignments were created using Clustal W (Thompson et al., 1994). Protein sequence alignments were performed with the following parameters: Gap opening penalty = 10.0, Gap extension penalty = 0.10 and Gonnet protein weight matrix. To reconstruct phylogenetic trees by maximum likelihood the multiple sequence alignments were analyzed with PHYML by submitting the alignments to the PHYML server (http://www.atgc-montpellier.fr/phyml) (Guindon et al., 2010). The LG substitution matrix was used for calculation of the amino acid substitutions (Le and Gascuel, 2008). A BIONJ distance-based tree was used as the starting tree to be refined by the maximum likelihood algorithm. The number of generated bootstrapped pseudo data sets was set to 100. The tree was drawn with Tree viewer at the T-REX web server (http://www.trex.uqam.ca/) (Alix et al., 2012). For the promoter analyzes 2000 bases upstream of the start codon in each LTPG sequence were used. The web tool "elefinder" at Matt Hudson Lab (http://stan.cropsci.uiuc.edu/tools.php) were used to identify cis-elements. The tool searches for overrepresented motifs in the promoter regions by comparing them to the *A. thaliana* genome. In this case the tool was used to find common motifs in the *P. patens* LTPG promoters.

2.3. Structural modeling

The 3D structural models of the lipid binding domains of PpLTPG2 and PpLTPG8 were constructed using the crystal structure of *A. thaliana* DIR1 (pdb code 2RKN; (Lascombe et al., 2008)) as a template. Firstly, a structure-based alignment of DIR1 and wheat LPT2 (pdb code 1TUK; (Hoh et al., 2005)) was made with VERTAA in BODIL (Lehtonen et al., 2004) and the PpLTPG2 and PpLTPG8 were then aligned to the fixed structure-based alignment with MALIGN in BODIL (Lehtonen et al., 2004). The crystal structure of DIR1 was chosen as a template for the modeling based on our previous studies (Edstam et al., 2011). MODELLER (Sali and Blundell, 1993) was used to create a set of ten 3D models for each sequence based on the crystal structure of DIR1 and the alignment between the sequence and the template. The best model of PpLTPG8 for future analysis was selected based on the lowest energy value of the MODELLER objective function. From the set of PpLTPG2 models, the one with the most similar backbone conformation to PpLTPG8 was chosen as a representative model.

The VADAR (version 1.8) webserver (http://vadar.wishartlab.com/) for single model protein structure analysis (Willard et al., 2003) was used to analyze the intramolecular hydrogen bonds formed in the PpLTPG2 and PpLTPG8 models, while the ProtParam tool at ExPASy (Gasteiger et al., 2005) was used to determine physical and chemical features of the target proteins including the amino acid composition of the proteins.

2.4. Gene expression analysis

To study the expression of LTPGs in *P. patens*, total RNA was extracted from 3 to 4 weeks old gametophytes or from liquid cultures using RNeasy Plant Mini Kit (Qiagen, Hilden, Germany), according to the protocol from the manufacturer. Liquid cultures were used for the treatments with abscisic acid (ABA), NaCl, mannitol and $CuSO_4$. Gametophytes in liquid cultures were shredded with a disperser (T18 Ultra-Turrax, IKA, Staufen, Germany) ahead of the treatment. During the treatments, the liquid cultures were grown at 25 °C under continuous light (6000 lux) with shaking (175 rpm). ABA, $CuSO_4$ and mannitol treatments were conducted for 24 h, and salt stress for 3 h. Moss cultures on agar were used for UV-B-, cold-, dark- and dehydration-treatments. The UV-B treatment was imposed by placing the petri dish upside-down, without the lid, on a UV-table (Spectroline, Bi-o-vision UV/White light transilluminator) at 280–315 nm for 1 h. For the cold treatment, the petri dish was placed on ice for 48 h. The dark treatment was

conducted by placing the plate in a light-proof box in the growth chamber for 24 h. Finally, the dehydration was imposed by removing the lid of the petri dish for 24 h, while keeping it in the growth chamber. For each treatment, three to five replicates were used, all treated independently. The purified RNA was treated with DNaseI (Invitrogen, Carlsbad, CA, USA). First strand cDNA was synthesized with RevertAid Reverse Transcriptase (Thermo Scientific) according to the protocol provided. The qRT-PCR was performed with Power SYBR Green PCR Master Mix (Applied Biosystems, Foster City, CA, USA) in a 25 μl reaction mixture according to the protocol supplied with the master mix. For each primer pair a standard curve was prepared to calculate the amplification efficiency of the primer pairs. Reactions were performed in triplicates from each RNA sample. Relative quantification of gene expression data was carried out with the $2^{-\Delta\Delta CT}$ or comparative CT method (Livak and Schmittgen, 2001). Expression levels were normalized with the CT values obtained for the housekeeping gene Pp*TUB1*, encoding β-tubulin 1 (Holm et al., 2010). For statistical evaluation of the results the obtained ΔCT-values were subjected to *t*-tests (Yuan et al., 2006). *P*-values below 0.05 are considered significant.

2.5. Histochemical GUS assays

Four genes encoding fusions between *P. patens* LTPGs and the β-glucuronidase (GUS) reporter gene were constructed and transformed to *P. patens*. The LTPG genes used were PpLTPG2, PpLTPG4, PpLTPG5 and PpLTPG8. To enable homologous recombination in *P. patens* two genomic DNA fragments from each gene were amplified using PCR with gene specific primers. Restriction sites were introduced to the sequences through the primers, to enable ligation into plasmids (Table S1). The right fragment, containing parts of the 3′UTR of the LTPG, was inserted between the NotI and XbaI sites of the plasmid pPpGUS (Eklund et al., 2010). The left fragment, containing a part of the coding region of the LTPG, was then ligated into the BamHI site of the same plasmid. Correct orientation of the left fragment was confirmed by both PCR and sequencing. Finally, the construct was cut out with XbaI and used for PEG-mediated transformation of moss protoplasts as described previously (Nishiyama et al., 2000). Both gametophores (leafy shoots) and protonema (filamentous tissue) were used in the GUS staining assay. A GUS staining solution containing 0.5 mM X-gluc, 0.5 mM $K_3Fe(CN)_6$, 0.5 mM $K_4Fe(CN)_6$, 0.01% Triton X and 50 mM NaH_2PO_4 (pH 7.0) was used. The samples were incubated in the stain for 48 h at 37 °C in darkness, and then fixed for 10 min in 5% formalin followed by 10 min in 5% acetic acid. After fixation the samples were dehydrated using increasing concentrations of ethanol, and finally put in glycerol for observation. Observations were done with a Nikon Elipse 80i microscope equipped with the digital camera Nikon DS-Fi1.

2.6. Transient expression of an YFP-PpLTPG2 fusion protein in *P. patens* and *N. tabacum*

A synthetic fusion gene of PpLTPG2 and YFP was ordered from Eurofin MWG Operon. For improving the success rate of DNA synthesis some nucleotide substitutions were done in PpLTPG2 without any consequent changes in the amino acid sequence. The synthetic gene encodes the N-terminal signal sequence of the PpLTPG2, followed by the YFP gene, a short linker and the actual PpLTPG2 open reading frame (ORF), including the C-terminal signal sequence that leads to the addition of the GPI-anchor (Figure S1). The plasmid psmRS-LY was constructed by inserting the synthetic construct as a BglII/SacI fragment between the 35S promoter and *NOS1* terminator in the psmRS-GFP plasmid (Davis and Vierstra, 1996; Edqvist et al., 2004) replacing the GFP gene which was released by BamHI/SacI-digestion. The plasmid psmRS-LY was transformed to moss protoplast. For transient expression of the YFP- PpLTPG2 fusion protein in *Nicotiana tabacum*, the cassette containing the YFP-LTP construct under the 35S promoter was released from the plasmid psmRS-LY by EcoRI/HindIII cleavage and inserted into the EcoRI/HindIII site of the binary vector pBI101 to obtain the vector pBILTP1. This plasmid was transformed into *Agrobacterium tumefaciens* strain C58 using freeze-thaw method (Chen et al., 1994) and grown on YM medium (yeast extract (0.4 g/l), Mannitol (10 g/l), NaCl (1.7 mM) $MgSO_4 \times 7H_2O$ (0.8 mM), $K_2HPO_4 \times 3H_2O$ (2.2 mM), pH 7.0) containing 50 μg/ml Kanamycin and 20 μg/ml Rifampicin. Transformation to *N. tabacum* (Impecta Fröhandel, Julita) was done as previously described (Sparkes et al., 2006). The plants were incubated under normal growing conditions for 4–5 days and then the infiltrated region was monitored. Localization of the YFP-PpLTPG2 fusion protein was studied in *P. patens* protoplasts and *N. tabacum* leaves with a Nikon Elipse 80i fluorescence microscope, equipped with the camera Nikon DS-Fi1 and an YFP filter (Brightline YFP-2427B-000, Semrock, Lake Forest, Illinois USA).

2.7. Expression and purification of heterologous proteins

PpLTPG2 and PpLTPG8 lipid binding domains were expressed in *Pichia pastoris* using the "EasySelect Pichia Expression Kit" from Invitrogen. The LTPG genes were amplified from moss cDNA using primers introducing an EcoRI site in the 5′-end and a NotI site in the 3′-end of the fragment to be cloned in frame of the α-factor, c-myc epitope and his-tag in the plasmid pPICZαA (Invitrogen). The fragments were cloned into the EcoRI/NotI site of pPICZαA and transformed into the *E. coli* strain Top10 F′ (Invitrogen) by electroporation (Micropulser, BioRad). Transformants were selected on low salt LB medium (1% tryptone, 0.5% yeast extract, 0.5% NaCl, pH 7.5) containing 25 μg/ml Zeocin (Life Technologies, Carlsbad, CA, USA). Plasmids were prepared using plasmid miniprep GeneJET kit (Thermo Scientific) and constructs were verified by restriction enzyme analysis and sequencing (Eurofins MWG Operon). The plasmids pPICZαA-LTPG2 and pPICZαA-LTPG8 were transformed as linear SacI cut fragments by electroporation into the *P. pastoris* strains KM71H and GS115 and grown at 30 °C on YPDS plates (1% yeast extract, 2% peptone, 2% glucose, 1 M sorbitol, 2% agar) containing 100 μg/ml zeocin. Verification of Mut^+ and Mut^S phenotypes and protein expression were done according to the instruction obtained with the EasySelect Pichia Expression Kit. When cells from the different *P. pastoris* strains were harvested the supernatant was separated from the cells by centrifugation at 1500 g for 5 min at 4 °C and stored in tubes at 4 °C until used. Protein production was monitored by western blot using an antibody towards the c-myc epitope in the C-terminal of the proteins. 10 μl of the supernatant was mixed with 10 μl loading buffer, heated 10 min at 100 °C and loaded onto a SDS-PAGE 4–20% gradient gel (Precise protein gels, Thermo Scientific). As molecular weight standard the PageRuler Plus prestained protein ladder was used (Thermo Scientific). Supernatants from the same *P. pastoris* strains expressing the same protein were pooled to a maximum volume of 50 ml and purified using HisGraviTrap (GE Healthcare) according to the suggested protocol from the manufacturer. The purification was done at 4 °C in buffers for native conditions. Protein concentrations were estimated by measuring A_{280} in a NanoDrop ND-1000 spectrophotometer (Thermo Scientific) or with the assay based on bicinchonic acid (BCA). The Pierce™ BCA Protein assay kit (Thermo Scientific) was used according to the instructions from the manufacturer.

2.8. Fluorescence lipid binding assay

A fluorescence based lipid binding assay of PpLTPG2 and PpLTPG8 was carried out using 6-(*p*-Toluidino)-2-naphthalenesulfonic acid (TNS) essentially as described previously (Buhot et al., 2004; Sawano et al., 2008). The excitation wavelength was set at 318 nm according to the fluorescence substrate TNS manufacturers' recommendations (Sigma–Aldrich) and emission wavelength was scanned between 370 and 600 nm with a scan speed of 1200 nm/min on an F-4500 Hitachi Fluorospectrophotometer. To determine the optimal concentration of TNS in relation to 1 μM protein an assay was set where TNS (1 mM in 10% DMSO) was added as aliquots from 0.1 μM to 30 μM in a 2 ml sample buffer (175 mM Mannitol, 0.5 mM K_2SO_4, 0.5 mM $CaCl_2$, and 5 mM MES at pH 7.0) containing 1 μM protein (PpLTPG2 or PpLTPG8) and measured in the emission interval 370–600 nm. Samples were measured at 25 °C and let to incubate 2 min after each addition of TNS. For the lipid binding assays a concentration of 20 μM TNS was chosen to 1 μM protein otherwise the sample conditions were the same as above. Each tested fatty acid was added in aliquots to the concentrations from 0.5 to 20 μM. Measurements were taken at fatty acid concentrations of 0.5, 2.5, 5, 7.5, 10, 15 and 20 μM. Each measurement was taken after thorough mixing and 2 min incubation. 5 measurements were taken at each point.

2.9. Circular dichroism spectroscopy

The secondary structures of the proteins were monitored using circular dichroism (CD) in the far UV from 190 to 260 nm at 25 °C on a Chirascan CD, Applied Photophysics. Proteins were transferred to a 20 mM K_2HPO_4/KH_2PO_4 pH 7 buffer by centrifugal concentration using Amicon Ultra concentrator columns according to the manufacturer's instructions. The proteins PpLTPG2 and PpLTPG8 were diluted to a concentration of 11 μM and 16 μM respectively in 20 mM K_2HPO_4/KH_2PO_4 pH 7.0 buffer for the spectral measurements. The spectra were expressed in terms of mean residue ellipticity (θ) (MRE) in degree cm^2 $dmol^{-1}$ from the ellipticity values in millidegrees (θ). The thermal induced unfolding of the proteins were monitored by changes in the ellipticity signal at 222 nm over an interval of 4–95 °C with a 1 °C step size and possible refolding were monitored over the same temperature interval reversed. Individual CD spectra were averaged over 10 scans with 0.5-nm increments using a 1 mm path length cuvette. The helical content (f) was calculated using the equation

$$f = -\frac{[\theta]_{obs} n}{40000(n-4)} \times 100$$

where n is the number of amino acids and θ is the observed ellipticity value at 222 nm (Lin et al., 2005). A second method, a web based program (http://dichroweb.cryst.bbk.ac.uk/html) from Dichroweb (Lobley et al., 2002; Whitmore and Wallace, 2004, 2008) was also used to estimate the helical content using the analysis method CDSSTR and the reference database 4 (Compton and Johnson, 1986; Manavalan and Johnson, 1987; Sreerama and Woody, 2000).

2.10. Polyester analysis

To determine the polyester content of cutin from *P. patens* gametophores a protocol developed for *A. thaliana* was used, with some modifications (Bonaventure et al., 2004). Approximately 2 g of gametophores were ground in liquid nitrogen and transferred to boiling isopropanol, where it was kept for 30 min, followed by incubation at room temperature for 2 h with constant shaking (300 rpm). The plant material was pelleted through centrifugation and the isopropanol removed. The pellet was resolved in chloroform:methanol 2:1 (v/v) and incubated for 2 h. The centrifugation step was repeated and the chloroform:methanol 2:1 was exchanged to chloroform:methanol 1:2 (v/v) and the sample was incubated overnight. This was followed by one more centrifugation, removal of the solvent and incubation in methanol for 2 h. The sample was then filtered to remove solvent, and the plant residues were dried in a vacuum desiccator for two weeks before depolymerization of cutin. Approximately 40 mg dry plant material was used in each reaction, and three replicates were done. Cutin was depolymerized through methanolysis with sodium methoxide, with C17:0 methyl ester and pentadecalactone as internal standards, followed by a silylation by BSTFA (Bonaventure et al., 2004). The lipid compositions of the samples were determined using a GC–MS equipped with a DB-5 capillary column (FactorFour, Varian, Palo Alto, CA, USA). Helium was used as carrier gas and the oven preheated to 100 °C. After injection (splitless) the temperature was hold at 100 °C for 1 min and then increased by 10 °C every min, up to 280 °C where it was constant for 20 min. Peaks were identified and relative peak areas calculated (after removal of internal standards).

3. Results

3.1. Conserved sequence elements in the moss LTPGs

In a previous study, it was shown that three of the 10 different sequences coding for LTPGs in *P. patens* had multiple 8CMs (Edstam et al., 2011). Both PpLTPG1 and PpLTPG5 contain two 8CMs and PpLTPG7 contains three 8CMs. For the sequence analysis these 8CMs were separated and designated as individual polypeptide chains in alphabetical order according to occurrence of the domain in the protein as PpLTPG1A and PpLTPG1B, PpLTPG5A and PpLTPG5B and PpLTPG7A, PpLTPG7B and PpLTPG7C. These 8CMs were then compared to the other seven LTPGs by ClustalW analysis (Fig. 1). The alignment is shown over the 8CM region omitting the signal peptide and keeping only four amino acids (aa) of the C-terminal sequences downstream of the 8CM. Except for the 8CM very few of the aa are conserved in all 14 8CMs from the eight LTPGs. Four additional aa are conserved in all sequences, namely a Leu three aa before Cys2, a Pro four aa before Cys3, a Pro two aa before Cys5 and an Asn eleven aa before Cys7. At four positions there are also conserved aa substitutions; an aromatic aa at three aa after Cys2, Leu/Val/Ile (in proportion 12/1/1 among the 14 sequences) between Cys5 and Cys6, a Leu/Ile (10/4) four aa before and a Leu/Val/Ile (1/10/3) two aa after Cys7. The spacing between the Cys in the 8CM are relatively fixed in all sequences, Cys1 and Cys2 are separated with nine aa (one exception of PpLTPG10 which has ten aa there), between Cys2 and Cys3 there are 14–16 aa, between Cys4 and Cys5 twelve aa, between Cys6 and Cys7 23–27 aa and between Cys7 and Cys8 seven aa. All these features could be a part of making the core structure of the LTPG in moss.

A higher similarity was found between the PpLTPG1, PpLTPG5 and PpLTPG7 proteins indicating a common origin for these proteins with multiple 8CMs. When the individual 8CMs from these proteins were aligned they all contain a conserved seven aa sequence PVCLCQI/L including Cys5 and Cys6. Between these three proteins, the N-terminal A 8CMs have the highest identity of 52% and the C-terminal B 8CMs together with the single C 8CM from PpLTPG7 have an identity of 32%. PpLTPG1A and PpLTPG5A have the highest identity with 80% identical amino acids. A phylogenetic tree (Fig. 1B) was reconstructed from the 8CM sequences using the maximum likelihood method. When looking at PpLTPG1, PpLTPG5 and PpLTPG7, the N-terminal A 8CMs from these proteins form a

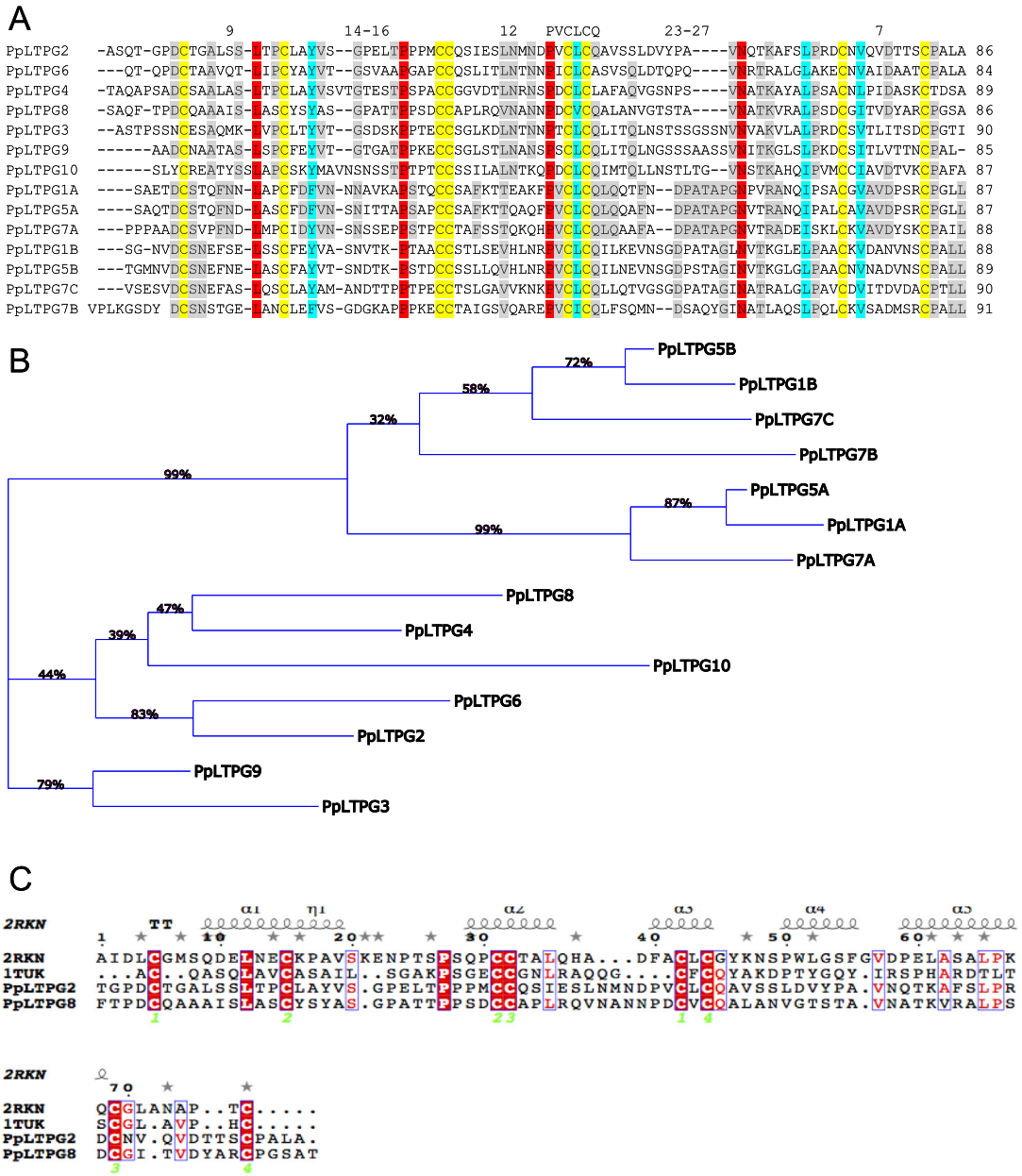

Fig. 1. Sequence analysis of *P. patens* LTPGs. In (A) is an aa sequence alignment of the 8CM region of the 10 LTPGs found in *P. patens*. Since PpLTPG1, PpLTPG5 and PpLTPG7 had more than one 8CM these motifs were individually compared and here named as an affix A, B or C in accordance to the occurrence of the motif in the protein. Motif with an A is defined closest to the N-terminal. The 8CM is marked in yellow, conserved residues found in all sequences in red and conserved substitutions in blue. The spacing between the Cys in the 8CM is shown at the top of alignment along with the signature PVCLCQ found in 7 motifs and partly conserved in the rest of the sequences. In (B) is a phylogenetic tree of *P. patens* LTPGs. The numbers indicate the percentage of 100 bootstrap re-samplings that support the inferred topology. The tree was constructed using the maximum likelihood method. In (C) the sequence alignment used for 3D modeling is shown. The A. thaliana DIR1 (2RKN) and wheat LPT2 (1TUK) structures were first superimposed and then the PpLTPG2 and PpLTPG8 sequences were aligned to the structure-based sequence alignment. The totally conserved positions are shown with red background and the conserved positions with red font. The secondary structure elements in the DIR1 structure are shown above the alignment and disulphides pairing indicated with green numbers under Cys residues. (For interpretation of the references to color in this figure legend, the reader is referred to the web version of this article.)

specific branch, while the B 8CMs together with the single C 8CM are grouped in a separate branch. It seems as if these multiple 8CM genes have evolved from a series of duplications, starting from one 8CM that was duplicated to give a gene encoding two 8CMs. Further duplications of this gene with two 8CMs resulted in the two additional genes encoding multiple 8CMs.

3.2. Moss LTPGs were successfully produced in P. pastoris

Two different strains, KM71H and GS115, of *P. pastoris* were transformed with constructs containing the PpLTPG2 or PpLTPG8 genes. Since heterologous protein levels vary between transformants, six transformants from each construct and strain were monitored for protein production by western blot. Fig. 2 shows the different expression levels of four transformants in GS115 containing the PpLTPG2 construct indicating an expression difference of tenfold between transformants. The coomassie stained gel indicated that homogenous LTPG fractions were obtained after affinity purification (Fig. 2B). When comparing expression levels in the different *P. pastoris* strains, GS115 gave a higher level compared to KM71H. GS115 gave an average production of 0.7 g/l of PpLTPG8 and 0.2 g/l of PpLTPG2 when the supernatant was harvested after 4

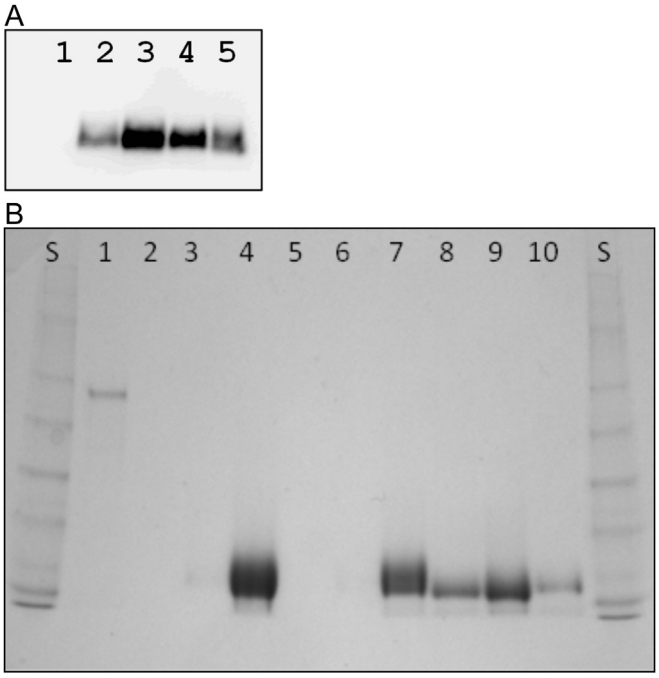

Fig. 2. Expression of PpLTPG2 and PpLTPG8 in the yeast *P. pastoris*. In (A) is a western blot of supernatants from growth media of *P. pastoris* GS115 transformants containing the PpLTPG2 protein. The protein is detected by antibodies towards the c-myc epitope attached to the PpLTPG2 protein. Lane 1 is supernatant from untransformed GS115 as a control and lane 2–5 are from 4 different transformants showing a variety of different expression levels of PpLTPG2. Similar results were obtained for *P. pastoris* GS115/PpLTPG8, *P. pastoris* KM71H/PpLTPG2 and *P. pastoris* KM71H/PpLTPG8. In (B) is a stained SDS-PAGE gel of PpLTPG2 and PpLTPG8 after purification and concentration from supernatants from the two different *P. pastoris* strains GS115 and KM71H. Lane 1 shows the 67 kD HSA protein from the supernatant expressed in the control strain GS115/Albumin at level >1 g/l (Invitrogen). Lanes 3, 4, 6 and 7 contain PpLTPG8 protein isolated from growth media from two different GS115 transformants. Lanes 8 and 9 carry PpLTPG8 isolated from growth media from two different KM71H transformants and lane 10 contain PpLTPG2 isolated from growth media from a KM71H transformant. Lanes 4, 7, 8, 9 and 10 show LTPG-protein (12 kD) which was first purified from the growth media using His-tag affinity purification and then concentrated using a filter protein concentrator. Lanes 3 and 6 carry protein samples before the concentration. No sample was added to lane 2 and 5. Similar results were obtained for *P. pastoris* GS115/PpLTPG2.

days of methanol induced growth. The KM71H were harvested after 8 days of methanol induction and gave an average production of 0.2 g/l of PpLTPG8 and 0.07 g/l of PpLTPG2.

3.3. The moss LTPGs are extremely heat stable

The 2D-structure and thermal stability of purified PpLTPG2 and PpLTPG8 were analyzed with circular dichroism (CD) spectroscopy. For both proteins, the results show an α-helical spectra with a double minima at 222 nm and 208 nm and a maximum at 195 nm (Fig. 3A). The helical content of the moss proteins were calculated to 30% in PpLTPG2 and 21% in PpLTPG8. When the proteins were subjected to heat denaturation they were both found to be very stable. PpLTPG8 did not denature during the heat treatment and the structure remained intact even at 95 °C suggesting an extremely stable protein (Fig. 3B). The PpLTPG2 protein remained an intact structure until 80 °C when it started to unfold and were fully denatured at 95 °C and could not be refolded by lowering the temperature (Fig. 3B). The Tm of PpLTPG2 was calculated to a very high value of 88 °C suggesting that even this protein has a very stable structure. A second CD measurement was done on the diluted proteins several weeks after the first measurements giving the exact same results, which also state the high stability of the proteins in low phosphate buffers.

3.4. PpLTPG8 has very high alanine content

Several factors have been reported to enhance thermal stability of proteins including increased number of salt bridges and hydrogen bonds, improved packing of protein core, shorter and tighter surface loops, better secondary structure propensities and oligomerization (Reviewed in Razvi and Scholtz (2006)). Moreover, it has been shown that certain amino acids are favored in thermophilic proteins depending on their 3D location (Reviewed in Zhou et al. (2008)). To find out the origin for the extremely high thermal stability of PpLTPG8, we constructed structural models of PpLTPG2 and PpLTPG8 and compared them with each other. The structural models of PpLTPG2 and PpLTPG8 both adopt the LTP2-like alpha-helical fold with hydrophobic ligand-binding cavity and there are no differences in the length of loops or secondary structure elements that would result in changes in thermal stability. The models were first analyzed with the VADAR (version 1.8) webserver for single model protein structure analysis (Willard et al., 2003). Special focus was set on the hydrogen bonds and salt bridges within PpLTPG2 and PpLTPG8 models, since these could be the reason for the differences in the thermostability. The VADAR analysis together with visual inspection of the models showed that there are no major differences in the hydrogen bonds or salt bridges. Next we calculated the amino acid composition of PpLTPG2 and PpLTPG8 with the ProtParam tool at ExPASy (Gasteiger et al., 2005) and analyzed the position of differing amino acids in the 3D models (Table 1 and Fig. 4). The most significant difference was noticed in the amount of Alas, which have been reported to be less frequent on the surface but more frequent in buried areas of thermophilic proteins compared to mesophilic ones (Pack and Yoo, 2004). The percentage of Alas in PpLTPG2 is 6.30%, which corresponds to five amino acids out of 79 in the modeled lipid-binding domain (Fig. 4A). On the contrary, PpLTPG8 is composed of 17.70% Alas corresponding to 14 residues out of 79. As a result, the difference is 11.40% and nine Alas. Three Alas are conserved between PpLTPG2 and PpLTPG8, seven polar (2Q, 2T, 2S, E) and four hydrophobic (G, L, V, M) residues in PpLTPG2 are replaced by Alas in PpLTPG8. The 14 Alas in PpLTPG8 are distributed all over the 3D structure and located both within helices and turns (Fig. 4B).

Additionally, PpLTPG8 has two more Args compared to PpLTPG2 and its three Args lie on the surface of the protein, which is in accordance with the fact that exposed Args are known to stabilize the surface parts of thermophilic proteins (Chakravarty and Varadarajan, 2000; Das et al., 2006; Kumar et al., 2000). The lack of Mets in PpLTPG8 might further stabilize its structure since Met is known as a thermolabile amino acid (Kumar et al., 2000; Xu et al., 2003). In general, the number of non-polar residues (G, A, V, I, L, M, P) is slightly higher (1.3%) and the number of polar amino acids (S, T, C, Q, N) is somewhat lower (−2.6%) in PpLTPG8 than PpLTPG2 as has been reported for other thermophilic proteins (Zhou et al., 2008). Consistent with the higher thermal stability, PpLTPG8 is more densely packed since the total volume of PpLTPG8 (8939.5 $Å^3$) is lower than that of PpLTPG2 (9308.3 $Å^3$).

3.5. Moss LTPGs prefer binding to unsaturated fatty acids

Next, we characterized the lipid binding capacity of the yeast-produced moss LTPGs. The dissociation constant, K_d, for PpLTPG2 or PpLTPG8 and the ligand TNS were determined by slowly increasing the concentration of TNS from 0.1 μM to 30 μM toward the fixed concentration of 1 μM of PpLTPG2 or PpLTPG8. The binding capacities of the proteins toward TNS were shown to be identical with a K_d of 5.6 μM (Fig. 5A). Fatty acids and a fatty acyl-CoA were chosen as ligands for competing against the TNS/PpLTPG complex. If the ligand competes and releases TNS from the LTPG,

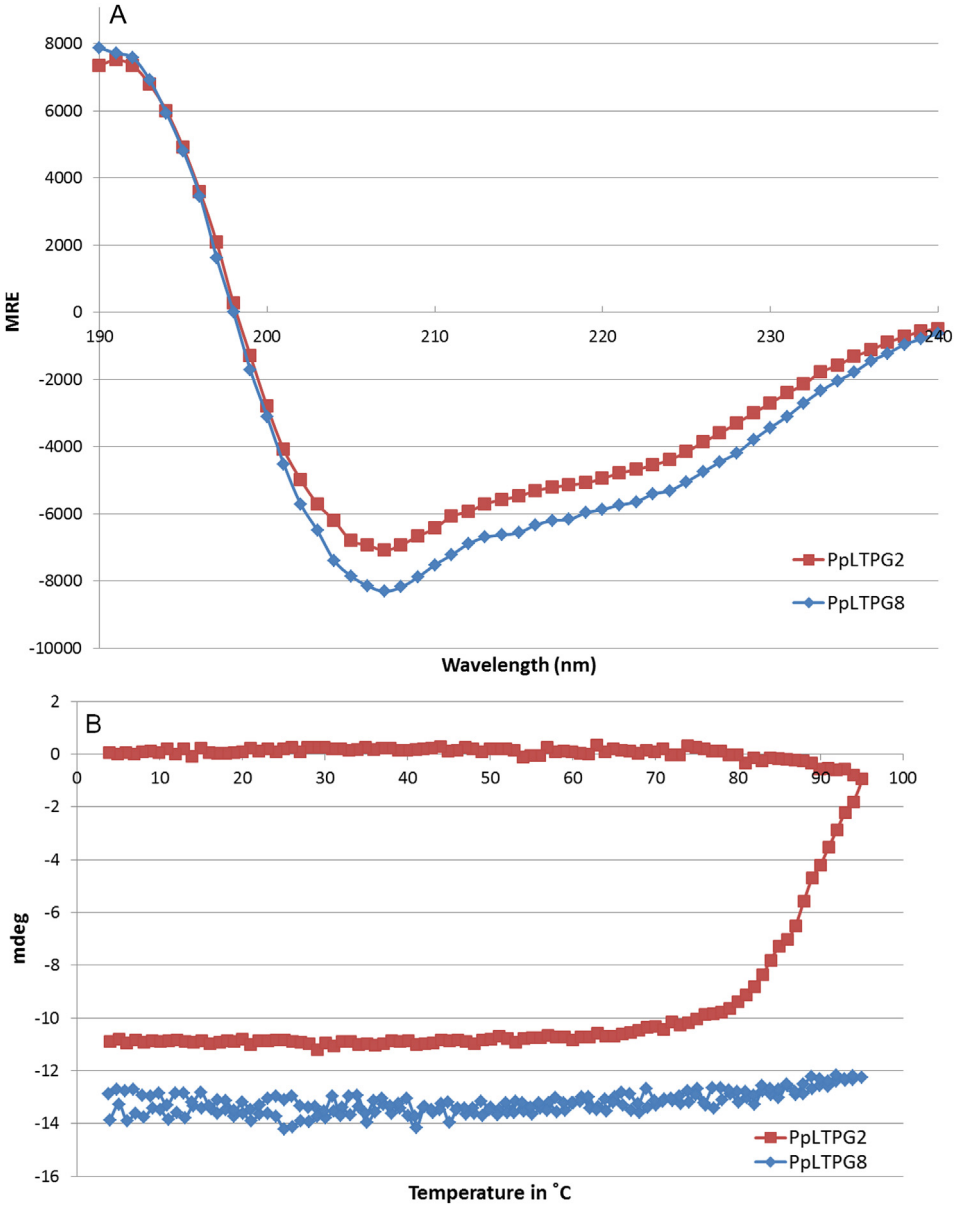

Fig. 3. CD analysis of PpLTPG2 and PpLTPG8. In (A) is the mean residue ellipticity (deg cm^2 mol^{-}) values in the far-UV spectra at 190–240 nm of PpLTPG2 and PpLTPG8 at 25 °C. In (B) is the thermal denaturation curves monitored by CD spectra at 222 nm.

the fluorescence is reduced. At 5 μM linoleic acid, the reduction of the LTP-TNS fluorescence was evident and reduced by 66% with both PpLTPG2 and PpLTPG8 (Fig. 5B). Oleic acid did slightly more efficiently displace TNS from PpLTPG2 compared to PpLTPG8, as fluorescence was reduced by 67% when binding to PpLTPG2 and 59% with PpLTPG8. With stearic acid a very low reduction was observed with 21% and 7% with PpLTPG2 and PpLTPG8, respectively. Stearoyl CoA reduced the fluorescence from TNS with 59% for both proteins.

To investigate the binding of PpLTPGs to very long-chain fatty acids, we also tested the competition assay with the hydroxylated fatty acid 22-hydroxydocosanoic acid. This is a common fatty acid found in suberin in vascular plants (Franke et al., 2005). The fluorescence level decreased step-wise with the subsequent additions of the fatty acid, indicating that 22-hydroxydocosanoic acid could compete with TNS for binding to the PpLTPGs (Fig. 5C). Compared with oleic and linoleic acid the fluorescence from TNS decreased much less, or with 20% at a concentration of 5 μM and to 40% at 20 μM. A plateau level for the fluorescence was never reached for competition with 22-hydroxydocosanoic acid as it was with linoleic acid and oleic acid. The binding competition with oleic acid is included for comparison in Fig 5C. Interestingly, after addition of oleic acid to the sample containing 20 μM 22-hydroxydocosanoic acid the fluorescence levels were continuing to decrease. The levels reached the plateau after the addition of 5 μM oleic acid (Fig. 5C). The reduction in fluorescence was never over 75% when higher concentrations of ligands were applied indicating that a fraction of TNS could not be outcompeted from binding to the LTPGs.

3.6. Cutin monomers were identified in P. patens

Following the lipid-binding assays we performed a lipid profiling of the leafy gametophores of *P. patens*. The results indicate the presence of a cuticle, or at least a cutin polymer. Both unsubstituted fatty acids, fatty alcohols and ω-hydroxylated fatty acids were represented among the monomers, mostly those with chain-lengths

Table 1
Amino acid analysis of PpLTPG2 and PpLTPG8. Features that might contribute to the higher thermal stability of PpLTP8 are shown in bold.

Amino acid	PpLTPG2		PpLTPG8		PpLTPG8-PpLTPG2
	Number of residues		Number of residues		% Difference
Ala A	**5**	6.30%	**14**	17.70%	**11.40%**
Arg R	**1**	1.30%	**3**	3.80%	**2.50%**
Asn N	4	5.10%	5	6.30%	1.20%
Asp D	5	6.30%	5	6.30%	0.00%
Cys C	8	10.00%	8	10.00%	0.00%
Gln Q	4	5.10%	3	3.80%	−1.30%
Glu E	2	2.50%	0	0.00%	−2.50%
Gly G	3	3.80%	3	3.80%	0.00%
His H	0	0.00%	0	0.00%	0.00%
Ile I	1	1.30%	2	2.50%	1.20%
Leu L	8	10.10%	4	5.10%	−5.00%
Lys K	1	1.30%	1	1.30%	0.00%
Met M	**2**	2.50%	**0**	0.00%	**−2.50%**
Phe F	1	1.30%	1	1.30%	0.00%
Pro P	9	11.40%	7	8.90%	−2.50%
Ser S	9	11.40%	7	8.90%	−2.50%
Thr T	7	8.90%	7	8.90%	0.00%
Trp W	0	0.00%	0	0.00%	0.00%
Tyr Y	2	2.50%	3	3.80%	1.30%
Val V	7	8.90%	6	7.60%	−1.30%
Properties					
Non-polar: GAVILMP		44.30%		45.60%	**1.30%**
Polar: STCQN		40.50%		37.90%	**−2.60%**
Polar-Charged: DERKH		11.40%		11.40%	0.00%

C_{16} to C_{18} (Table 2). The unsubstituted fatty acids constitute the largest class, with 70% of the total monomer content. This is a higher amount compared to the composition in other plants, where the content of those normally ranges between 0 and 25% (Pollard et al., 2008). Among the unsubstituted fatty acids in *P. patens* C_{16} to C_{18} are the major constituents, but C_{20}, C_{22} and C_{24} are found as well. In other studied plants only C_{16} and C_{18} are found in cutin, but longer chain-lengths are found in suberin (Pollard et al., 2008). Further, unsaturations were found among the unsubstituted fatty acids C_{18} and C_{20}. Both mono- and di-unsaturated C_{18} are common cutin monomers in plants, while the tetra-unsaturated C_{20} have never been reported before. This fatty acid is usually not found at all in plants, except for some mosses and ferns (Schlenk and Gellerman, 1965; Anterola et al., 2009). Only one fatty alcohol was found, C_{18}-1-ol, and in very small amount (1.34% in one sample, not at all in the others). Further, there was a large amount (<6%) of a triol, also with chain-length C_{18}. Among the hydroxylated fatty acids on the other hand, only C_{16} were found. There was a small amount (~2.6%) of the ω-hydroxylated C_{16} and a very large amount (24%) of the di-hydroxylated C_{16}. The C_{16} hydroxylated fatty acids are the main cutin monomers in most plants. There were no dicarboxylated fatty acids found in the moss samples. This class constitutes about 50% of the total cutin monomer content in *A. thaliana*, but is much lower in other plants (Franke et al., 2005; Pollard et al., 2008).

In addition to the cutin monomers several alkanes were found in the analysis of one of the three samples (Table 3). This is probably residues of the cuticular waxes. The results may not be complete, since these compounds were supposed to be removed during the preparation of the sample. Anyhow, the results indicate that most of the very long-chain alkanes (C_{25}–C_{33}) usually found in the cuticular wax layer are present in *P. patens* as well.

3.7. The moss LTPGs localize to the cell periphery

To investigate where the moss LTPG proteins are localized in the plant cell, a fusion protein of PpLTPG2 and YFP was constructed. In this construct the fusion protein had the intact N-terminal and C-terminal signal sequences from PpLTPG2. According to PROSITE (http://prosite.expasy.org/) (Sigrist et al., 2010) this N-terminal sequence has a 92% probability to transfer the protein to the plasma membrane and the C-terminal sequence an 85% probability of giving an addition of a GPI anchor. Moss protoplasts were transformed with the fusion protein and visualized under an epifluorescence microscope. The fusion protein was targeted to the plasma membrane giving a brightly fluorescent plasma membrane compared to the untransformed cells (Fig. 6A). To see whether the fusion protein would be targeted in a plant with an intact cell wall the PpLTPG2-YFP fusion was further transiently expressed in *N. tabacum* (Fig. 6B). In *N. tabacum* leaves, the fusion protein was targeted to the plasma membrane.

3.8. Many promoter cis-elements are conserved between moss and A. thaliana LTPGs

Analyzes of promoter sequences from LTPG genes in *P. patens* revealed that eleven known cis-elements are common among the genes (Table 4). Five of the identified cis-elements (Ibox, SORLIP1, SORLIP2, SORLIREP3 and T-box) are involved in light-regulated gene expression (Chan et al., 2001; Hiratsuka and Chua, 1997;

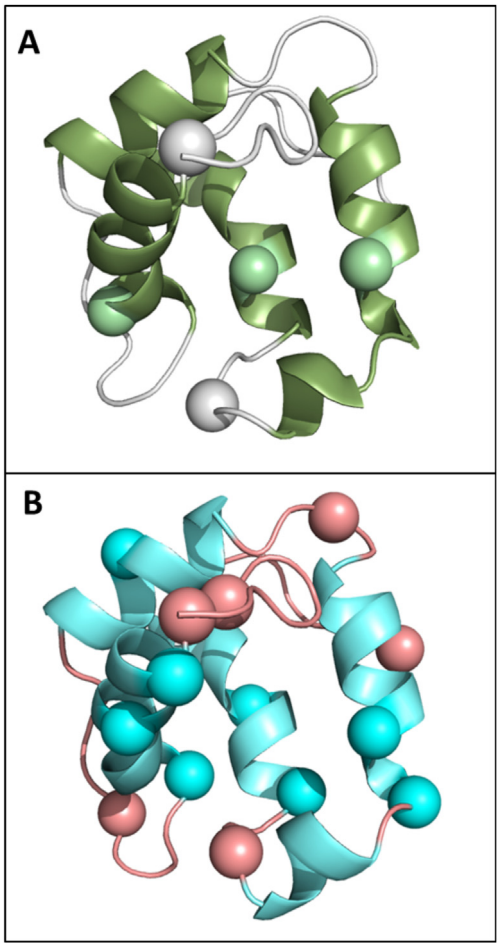

Fig. 4. Distribution of Alas in the 3D models of PpLTPG2 (A) and PpLTPG8 (B). The 14 Alas in PpLTPG8 are spread all over the lipid-binding domain and only three of them are conserved in PpLTPG2. (A) The 3D fold PpLTPG2 is shown as a cartoon with green helices and gray loops. Alas as spheres with the same color-coding. (B) The 3D fold of PpLTPG8 is presented with cyan helices and pale pink loop areas. Alas are shown as spheres with the same color-coding. (For interpretation of the references to color in this figure legend, the reader is referred to the web version of this article.)

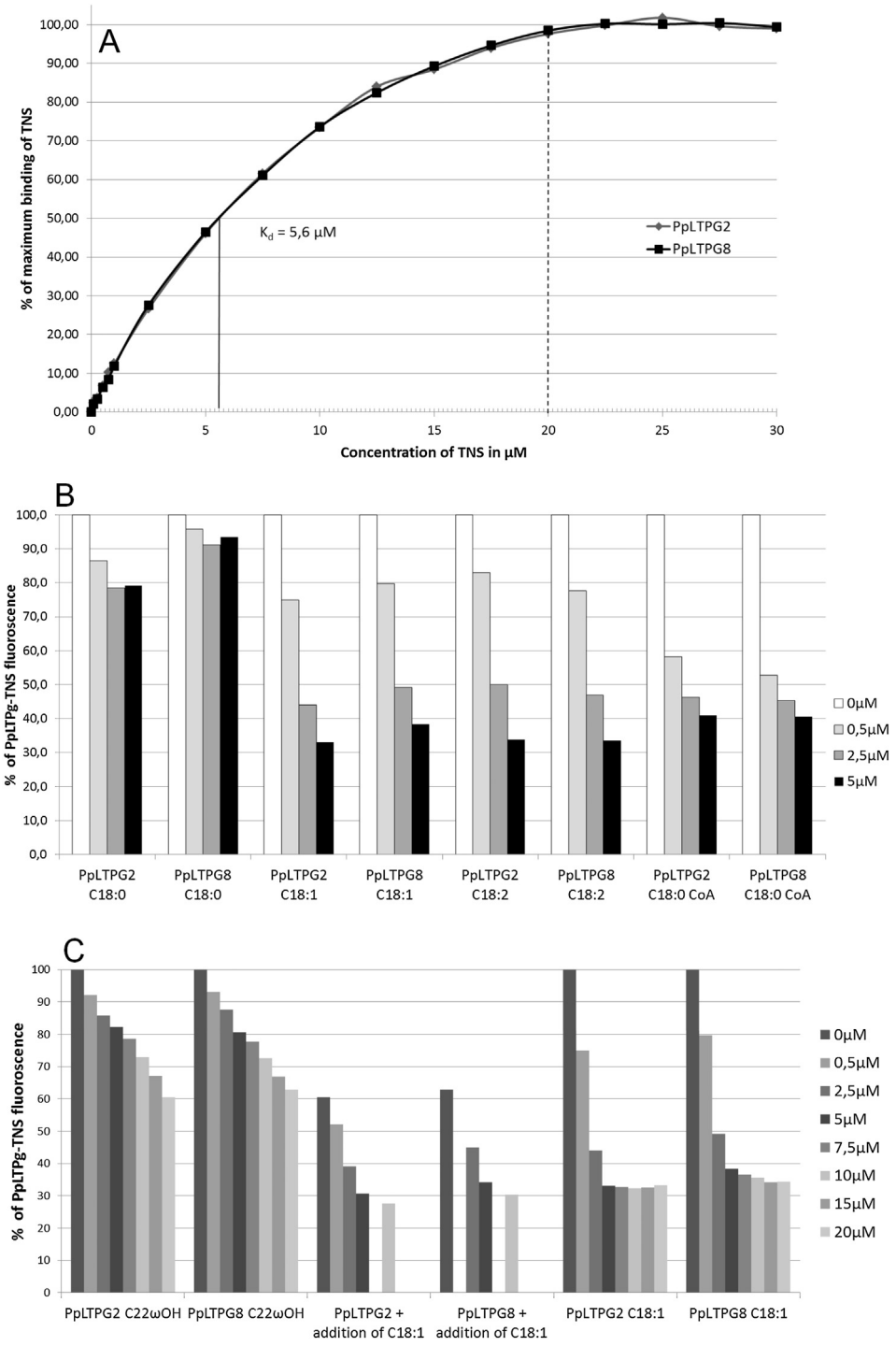

Fig. 5. Lipid binding of PpLTPG2 and PpLTPG8. Affinity measurements (A) of PpLTPG2 and PpLTPG8 to the ligand TNS recorded by an increase of fluorescence. The concentration of TNS was increased from 0.1 µM to 30 µM in aliquots. The results are presented as the percentage of maximum binding of TNS. This 100% value was obtained by calculating the average fluorescence for the TNS concentrations 22.5, 25, 27.5 and 30 µM. In (B) is the ability of different C18-fatty acids and fatty acyl-CoA to compete with TNS for binding to PpLTPG2 or PpLTPG8. This is shown by the reduction of fluorescence from the PpLTPG/TNS complex. In (C) is the binding to PpLTPG of the very long chain fatty acid 22-hydroxydocosanoic acid monitored at a concentration of 0.5–20 µM (leftmost set of bars). The center set of bars show a continuing decrease if oleic acid is added in the concentrations indicated to the 22-hydroxydocosanoic acid/TNS/PpLTPG8 complex. Included as a comparison, is the rightmost set of bars which are showing PpLTP binding when only oleic acid is added in concentrations from 0.5 to 20 µM.

Hudson and Quail, 2003). The RAV1-B element is important for leaf senescence in *A. thaliana* and therefore at least indirectly connected to photosynthesis (Fowler and Thomashow, 2002; Hu et al., 2004; Woo et al., 2010). The remaining five identified cis-elements (AtMYC2, DPBF, LTRE, DRE-like, LTRE and W-box) are connected to responses to environmental stresses (Abe et al., 1997; Chen et al., 2002; Dunn et al., 1998; Kim et al., 1997). The AtMYC2 binding site is found in genes involved in responses to dehydration. This cis-element was found in all analyzed PpLTPG promoters. Our expression analysis also revealed that several of the *P. patens* LTPG

Table 2
Cutin monomers found in *P. patens*.

Unsubstituted fatty acids		
C16:0	38.21%	±3.9
C18:0, C18:1, C18:2	21.19%	±1.7
C20:0	2.56%	±0.72
C20:4	2.70%	±0.47
C22:0	2.03%	±0.4
C24:0	2.62%	±0.95
Total unsubstituted	69.31%	±5.18
Fatty alcohols		
C18OH	1.34%	±1.3
Triols		
C18−3OH	6.25%	±1.6
Hydroxylated fatty acids		
C16ωOH	2.60%	±0.38
C16ω2OH	21.40%	±3.9
Total hydroxylated	24.00%	±4.1

genes were significantly upregulated during dehydration. The DRE-like and LTRE cis-elements are related to gene expression induced in low-temperatures. Interestingly, all but two (DRE-like and SORLIP2) of the eleven identified cis-elements were previously found to be enriched in the promoter sequences of LTPG genes from *A. thaliana* (Edstam et al., 2013) This suggests that mechanisms controlling the expression of LTPG genes may, at least to some extent, be conserved between mosses and flowering plants.

3.9. Dehydration induce the expression of many P. patens LTPGs

The expression level of eight of the *P. patens* LTPG genes were examined during several different conditions (Fig. 7). As expected from the search of regulatory cis-elements, cold and dehydration were found to cause a significant upregulation of several *P. patens* LTPG genes. After cold treatment three genes are significantly upregulated (PpLTPG3, PpLTPG8 and PpLTPG9), while one (PpLTPG5) is downregulated. Both DRE-like and LTRE cis-elements were identified in the promoter of PpLTPG8. Dehydration causes a significant upregulation of four genes (PpLTPG2, PpLTPG3, PpLTPG6 and PpLTPG9). Treatment of the moss with UV-B radiation, ABA, salt, mannitol and Cu^{2+} lead to downregulations of the PpLTPG genes. The only significant upregulation with these treatments was found for PpLTPG2 after treatment with mannitol. Growth in darkness did not affect the expression of any of the studied LTPG genes.

Furthermore, to get detailed information about the tissue specificity of the PpLTPG promoters we fused DNA-fragments carrying the promoters as well as the ORFs of PpLTPG2, PpLTPG4, PpLTPG5 and PpLTPG8 to the reporter gene β-glucuronidase (GUS). These gene fusions were transformed to *P. patens* and the selected, stable transformants were checked for GUS-activity. The GUS staining assay revealed weak expression of the PpLTPG2-GUS fusion in the midribs of the leafy gametophores. A stronger signal was seen in the tips of developing protonemal tissues (Fig. 8A). PpLTPG4-GUS is highly expressed in the gametophores, and particularly abundant in the midribs. The gene is expressed evenly over the whole leafy structure. The PpLTPG4 promoter is also very active in protonema (Fig. 8B) and rhizoids (not shown). PpLTPG5-GUS is expressed in the leafy gametophores. The expression is concentrated to the base of the leafy structure, and much weaker at the tip of the gametophore (Fig. 8C). The PpLTPG5 promoter is not active in protonemal tissues. PpLTPG8-GUS is expressed in midribs and developing rhizoids, but not in protonema (Fig. 8D). In summary, each PpLTPG show a characteristic expression pattern in the moss tissues.

Table 3
Alkanes found in *P. patens*.

Alkane	Relative amount
C22	5.88%
C23	6.83%
C24	9.32%
C25	13.60%
C26	14.79%
C27	13.32%
C28	11.51%
C29	10.21%
C30	6.96%
C31	5.15%
C32	2.43%

4. Discussion

All LTPGs from *P. patens* have a hydrophobic Leu, Val or Ile between Cys5 and Cys6 suggesting a 3D-structure and binding cavity similar to the LTP2-fold. The hydrophobic residue between Cys5 and Cys6, preferably a Leu, Val or Ile, is also conserved in *A. thaliana*, rice, *Pinus taeda*, *M. polymorpha* and *Selaginella moellendorffii* (Edstam et al., 2011). Thus, LTPGs have the LTP2-type of 8CM with disulfide parings between Cys residues 1–5, 2–3, 4–7 and 6–8. Both the PpLTPG2- and the PpLTPG8-proteins were found to be very thermally stable where PpLTPG2 had a Tm of 88 °C and PpLTPG8 could not be denatured by temperatures up to 95 °C. In previous investigations, nsLTPs from higher plants such as LTP1 from barley (*Hordeum vulgare* L.) and apple (*Malus domestica*) (Lindorff-Larsen and Winther, 2001; Sancho et al., 2005) were also shown to be very resistant to thermal inactivation. However, an nsLTP from peach (*Prunus persica*) was thermolabile at pH7 but more stable at pH3 (Gaier et al., 2008) whereas a sunflower (*Helianthus annuus* L.) nsLTP was found to have an intermediate thermostability showing some conformational alterations after heating to 80 °C (Berecz et al., 2010). Thus, most nsLTPs have an extreme thermal stability, although it is clear that there are also examples of nsLTPs with lower stability in high temperatures. Based on the amino acid composition and 3D structure analysis, the higher frequency of Alas and surface Args together with the lower frequency of Mets could account for the higher thermal stability of PpLTPG8 compared to that of PpLTPG2. The large amount of exposed Alas is known as a characteristic feature of thermophilic proteins, since the short alkyl group of Alas may interact more closely with neighboring residues resulting in a better packed protein structure (Pack and Yoo, 2004). The fact that Ala of all amino acids is the best helix-former (Argos et al., 1979) further supports the role of the high number of Alas in the high thermal stability of PpLTPG8.

Both PpLTPG2 and PpLTPG8 showed a preference for unsaturated C18 fatty acids. Similar results have been obtained for nsLTPs from *Ginkgo biloba* and *N. tabacum* (Buhot et al., 2004; Sawano et al., 2008). Thus, seemingly linear saturated fatty acids are not as easily fitted in the hydrophobic binding cavity of these nsLTPs. On the other hand, in earlier experiments maize (*Zea mays*) and wheat (*Triticum aestivum*) nsLTPs showed decreasing affinities with increasing number of unsaturation in C18 fatty acids (Zachowski et al., 1998; Guerbette et al., 1999). The competition assay further revealed that the moss LTPGs were more readily binding to stearoyl CoA compared to stearic acid. In contrast, the binding to maize nsLTP was only slightly affected when coenzyme A was esterified to the fatty acid (Zachowski et al., 1998). However, binding studies with barley nsLTPs also demonstrated that acyl-CoA esters were binding more tightly than the corresponding fatty acids (Lerche and Poulsen, 1998). As suggested by Lerche and Poulsen (1998), this could be due to that the acyl-CoA esters more resemble the long acyl monomers necessary for cutin biosynthesis. However, in our

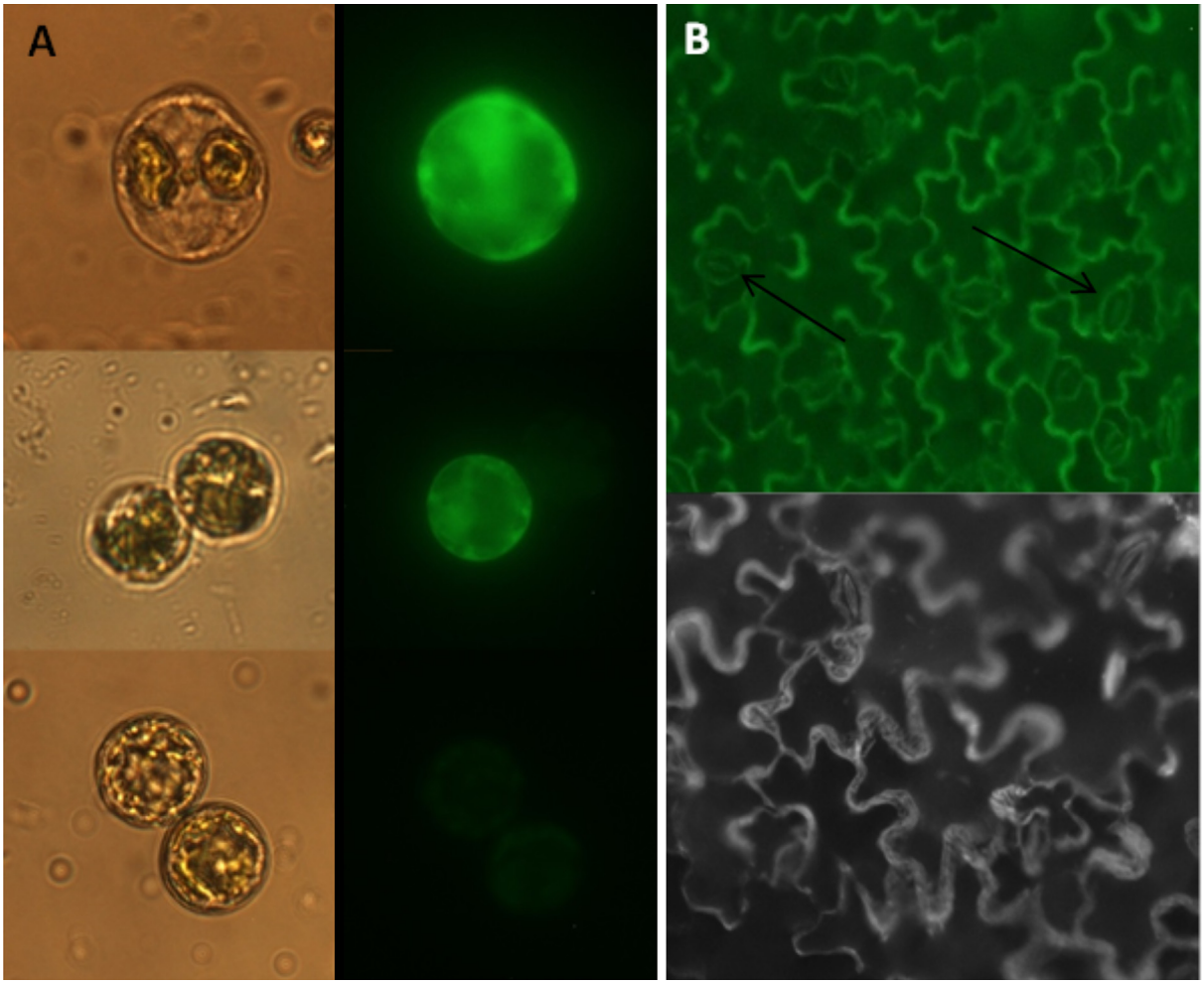

Fig. 6. Localization of PpLTPG2. The YFP-PpLTPG2 fusion protein was expressed in *P. patens* protoplasts (A) and in *N. tabacum* leaves (B). In (A) the top panel shows a *P. patens* transformant where the YFP-PpLTPG2 protein is shown to be targeted to the plasma membrane, the less glowing hollow circles are the less fluorescent chloroplasts. The middle panel shows a transformant next to an untransformed protoplast. The bottom panel shows two untransformed protoplasts where the chloroplasts can be visualized through slightly auto fluorescence. The pictures on the left hand side show the protoplasts under visible light where the chloroplasts can be visualized. In (B) is the localization of the fusion protein YFP-PpLTPG2 to the plasma membrane in *N. tabacum* leaves. The bottom panel in (B) shows a black and white picture in higher resolution. Arrows are pointing at guard cells.

experiments 22-hydroxydocosanoic acid was found to compete with less efficiency for binding to the PpLTPGs than oleic acid, linoleic acid and stearoyl CoA. Thus, we did not find evidence that very long chains would be more easily accommodated in the hydrophobic binding cavity of the PpLTPGs. We should point out that we have only tested one hydroxylated very long chain fatty acids in the competition. It is still possible that the PpLTPGs bind efficiently to other types of very long-chain fatty acids. However, also maize nsLTP displayed decreasing affinities for fatty acids with carbon chain over 18 carbons (Zachowski et al., 1998).

When the expression patterns of the PpLTPG genes were monitored during stress most treatments caused a downregulation of the genes. However, drought caused a significant upregulation of PpLTPG2, PpLTPG3, PpLTPG6 and PpLTPG9. Drought is also upregulating the expression of nsLTPs in *A. thaliana* and rice (Guo et al., 2013a,b). Interestingly, many of the cis-elements identified in the moss promoters were also previously identified in *A. thaliana* (Edstam et al., 2013). Seemingly, the regulatory circuits controlling the nsLTP expression are to a rather large extent conserved between mosses and flowering plants.

One of the hypotheses regarding nsLTPs in flowering plants is that they have a function in the synthesis or deposition of cutin and cuticular wax. This was first based on the abundance of nsLTPs in epidermis. More recently, results from nsLTP-knockout or knockdown plants have also pointed in that direction. Whether land plants from early diverging lineages have a cuticle or cuticle-like structures have been rather unclear and disputed. A multilayered cuticle, similar in structure to the cuticle in flowering plants, was recently shown on the maternal gametophytic calyptra in the moss *Funaria hygrometrica* by scanning and transmission electron microscopy (Budke et al., 2011]). A cuticle with similar chemical structure, but with less layers and complexity than that of vascular plants, occurs on other moss organs, including sporophytes and thalloid gametophytes (Neinhuis and Jetter, 1995; Cook and Graham, 1998). The cuticle in early diverging plant could serve an important function in protecting the plants from dehydration (Budke et al., 2013). In this study, we performed a lipid profiling of the leafy gametophores of *P. patens* and could identify known cutin and wax monomers, such as ω-hydroxylated fatty acids, fatty alcohols and long-chain alkanes. Our results indicate that there is a cuticle or a cuticle-like structure also in *P. patens*. This was also supported in another recent study (Buda et al., 2013).

To summarize, in this investigation we show that the moss gametophytes have a cuticle or cuticle-like structure, the C18 fatty acids amounts are high among the *P. patens* cutin monomers and the PpLTPGs have high affinity for C18 fatty acids: Furthermore, we found out that PpLTPGs localize to the cell periphery and are upregulated during drought stress. These findings indicate that also

Table 4
Identified cis-regulatory promoter elements in the PpLTPG genes from *P. patens*. Only cis-elements identified in at least four different genes are shown.

Promoter motif	Genes with the motif found in promoter	Description	References
AtMYC2	All ten PpLTPGs	Dehydration- and ABA-induced gene expression	Abe et al. (1997)
DPBF1&2	All ten PpLTPGs	ABA-responsive and embryo-specification elements	Kim et al. (1997)
DRE-like	PpLTPG2, PpLTPG4, PpLTPG5, PpLTPG8, PpLTPG10	Response to environmental stresses	Chen et al. (2002)
Ibox	PpLTPG1, PpLTPG3, PpLTPG4, PpLTPG5, PpLTPG6, PpLTPG7, PpLTPG8, PpLTPG10	Light-regulated gene expression	Hiratsuka and Chua (1997)
LTRE	PpLTPG2, PpLTPG4, PpLTPG8, PpLTPG10	Low-temperature-induced	Fowler and Thomashow (2002), Hu et al. (2004), Woo et al. (2010)
RAV1-B binding site	PpLTPG2, PpLTPG3, PpLTPG5, PpLTPG6, PpLTPG7, PpLTPG8, PpLTPG10	Leaf senescing, growth, cold	Hudson and Quail (2003)
SORLIP1	All ten PpLTPGs	Light-regulated gene expression	Hudson and Quail (2003)
SORLIP2	PpLTPG1, PpLTPG2, PpLTPG3, PpLTPG5, PpLTPG6, PpLTPG8, PpLTPG10	Light-regulated gene expression	Hudson and Quail (2003)
SORLREP3	PpLTPG1, PpLTPG3, PpLTPG4, PpLTPG10	Light-regulated gene expression	Hudson and Quail (2003)
T-box	PpLTPG1, PpLTPG2, PpLTPG3, PpLTPG4, PpLTPG5, PpLTPG6, PpLTPG8, PpLTPG9, PpLTPG10	Light-regulated gene expression	Chan et al. (2001)
W-box	PpLTPG1, PpLTPG2, PpLTPG3, PpLTPG5, PpLTPG6, PpLTPG7, PpLTPG8, PpLTPG9, PpLTPG10	Defense response	Chen et al. (2002)

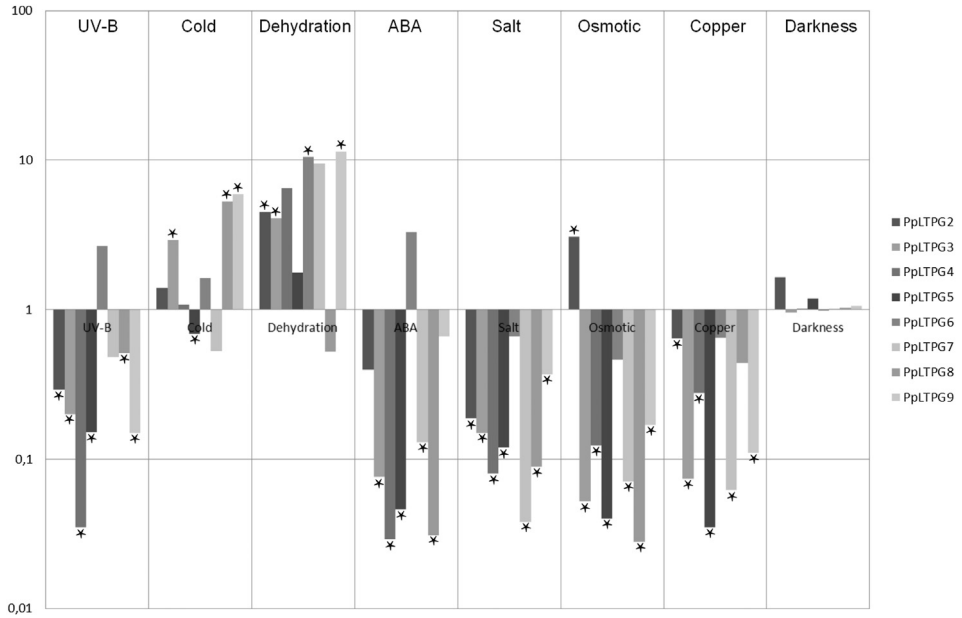

Fig. 7. Transcriptional regulation of eight *P. patens* LTPGs. The diagram shows the relative expression levels measured with qRT-PCR. The expression level of the control, grown under normal growth conditions, was set to one. Values below one indicate a down regulation, while values above one indicate an up regulation of the gene. Significant changes ($P < 0.05$) in expression level are indicated by a star.

moss PpLTPGs could be involved in the synthesis or deposition of cutin and cuticular wax.

5. Conclusions

We have shown that nsLTPs from mosses share many features with nsLTPs from flowering plants, such as extreme thermal stability, similar cellular localization and ligand binding preferences, as well as related regulatory mechanisms. It therefore seems plausible that moss nsLTPs are involved in related biological processes as the nsLTPs from flowering plants. We speculate that the GPI-anchored nsLTPs are involved in the development of the cuticle also in mosses. One function of these proteins could be to manage the transport of the hydrophobic cutin and wax monomers through the hydrophilic cell wall. We also note that the tissue specific expression patterns shown for PpLTPGs could mean that the individual proteins may have specialized functions covering several biological processes. Further studies with additional tools may provide us with answers regarding the detailed functional mechanisms of the enigmatic nsLTPs.

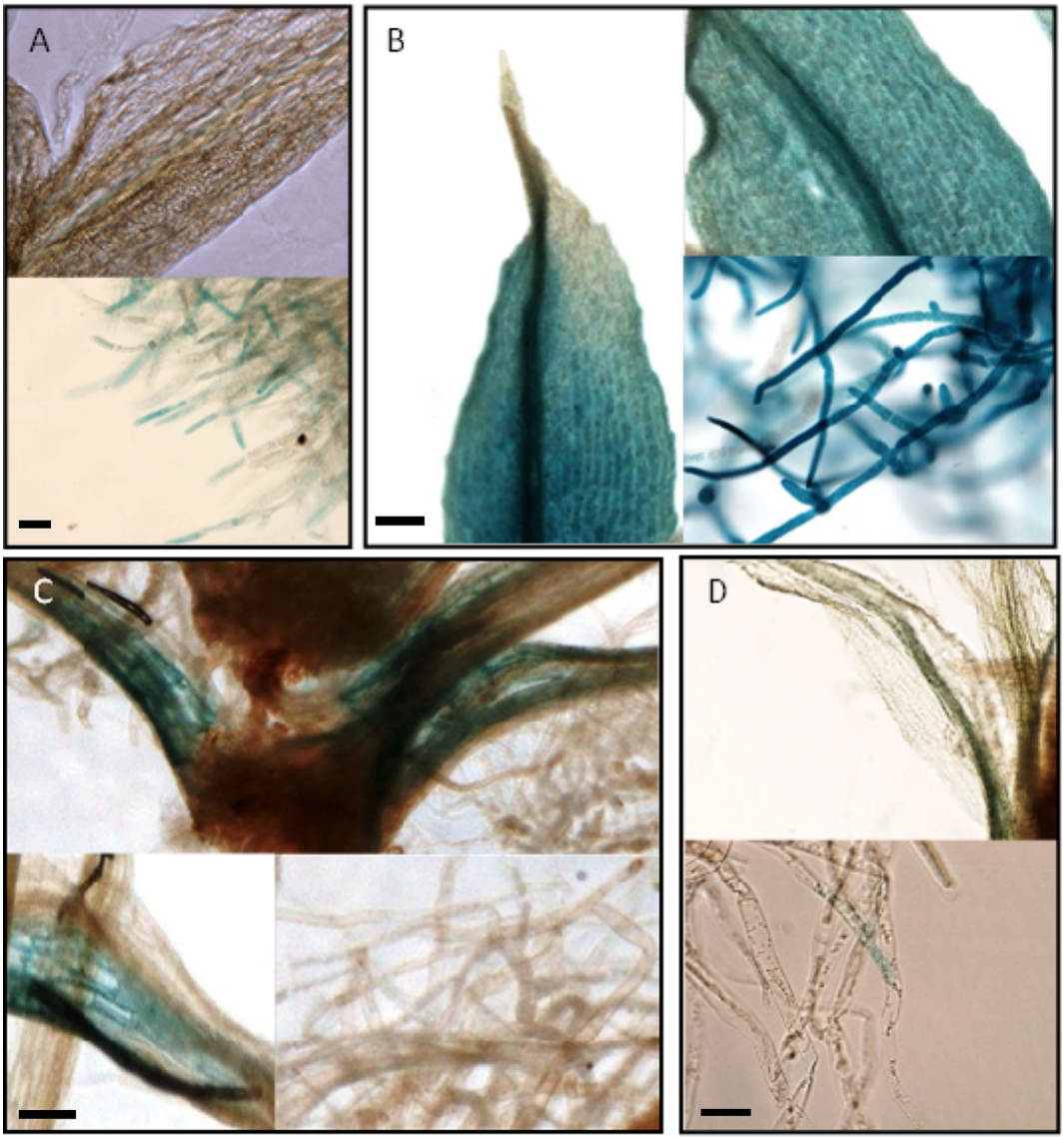

Fig. 8. Localization of GUS protein in transgenic *P. patens* plants expressing GUS from PpLTPG promoters. The GUS expression was observed in gametophores and protonema transgenic plants when GUS was under the regulation of the PpLTPG2 promoter (A), PpLTPG4 promoter (B), PpLTPG5 promoter (C) or PpLTPG8 promoter (D). The size bars represent 0.1 mm.

Acknowledgments

The authors are grateful for the advice and assistance on moss cultivation and transformation from Mattias Thelander and Magnus Eklund. We thank Sandra Jansson for help with the gene expression analysis, Sara Helander and Cecilia Andrésen for assistance with CD- and fluorescence-spectrometers, and Elke Schweda and Johan Dahlén for assistance with the GC–MS. We also thank Professor Mark Johnson for the excellent computing facilities at the Structural Bioinformatics Laboratory at Department of Biosciences at Åbo Akademi University. Use of Biocenter Finland infrastructure at Åbo Akademi (bioinformatics, structural biology, and translational activities) is acknowledged, along with the National Doctoral Program in Informational and Structural Biology. This work was supported by Carl Tryggers Stiftelse, Sigrid Juselius Foundation, Tor Joe and Pentti Borgs Foundation, and Åbo Akademi Graduate School

Contributions

MME performed and wrote GUS-stainings, qRT-PCR and promoter-studies, ML and KMD performed and analyzed modeling, AH performed qRT-PCR, AR performed parts of the Pichia-expression, TA designed, analyzed and wrote structural modeling, JE designed, analyzed and wrote research, KB designed, performed, analyzed and wrote Pichia-expression, ligand-binding assays, CD-analysis, LTPG-YFP localization and sequence-analysis.

Appendix A. Supplementary data

Supplementary data related to this article can be found at http://dx.doi.org/10.1016/j.plaphy.2013.12.001.

References

Abe, H., Yamaguchi-Shinozaki, K., Urao, T., Iwasaki, T., Hosokawa, D., Shinozaki, K., 1997. Role of arabidopsis MYC and MYB homologs in drought- and abscisic acid-regulated gene expression. Plant Cell 9, 1859–1868.

Alix, B., Boubacar, D.A., Vladimir, M., 2012. T-REX: a web server for inferring, validating and visualizing phylogenetic trees and networks. Nucleic Acids Res. 40, W573–W579.

Anterola, A., Gobel, C., Hornung, E., Sellhorn, G., Feussner, I., Grimes, H., 2009. *Physcomitrella patens* has lipoxygenases for both eicosanoid and octadecanoid pathways. Phytochemistry 70, 40–52.

Argos, P., Rossmann, M.G., Grau, U.M., Suborn, H., Frank, G., Tratschin, J.D., 1979. Thermal stability and protein structure. Biochemistry 18, 5698–5703.

Berecz, B., Mills, E.N., Tamás, L., Láng, F., Shewry, P.R., Mackie, A.R., 2010. Structural stability and surface activity of sunflower 2S albumins and nonspecific lipid transfer protein. J. Agric. Food Chem. 58, 6490–6497.

Bonaventure, G., Beisson, F., Ohlrogge, J., Pollard, M., 2004. Analysis of the aliphatic monomer composition of polyesters associated with Arabidopsis epidermis: occurrence of octadeca-cis-6, cis-9-diene-1,18-dioate as the major component. Plant J. 40, 920–930.

Boutrot, F., Chantret, N., Gautier, M.F., 2008. Genome-wide analysis of the rice and Arabidopsis non-specific lipid transfer protein (nsLtp) gene families and identification of wheat nsLtp genes by EST data mining. BMC Genom. 9, 86.

Buda, G.J., Barnes, W.J., Fich, E.A., Park, S., Yeats, T.H., Zhao, L., Domozych, D.S., Rose, J.K., 2013. An ATP binding cassette transporter is required for cuticular wax deposition and desiccation tolerance in the moss *Physcomitrella patens*. Plant Cell. http://dx.doi.org/10.1105/tpc.113.117648.

Budke, J.M., Goffinet, B., Jones, C.S., 2011. A hundred-year-old question: is the moss calyptra covered by a cuticle? A case study of *Funaria hygrometrica*. Ann. Bot. 107, 1279–1286.

Budke, J.M., Goffinet, B., Jones, C.S., 2013. Dehydration protection provided by a maternal cuticle improves offspring fitness in the moss *Funaria hygrometrica*. Ann. Bot. 111, 781–789.

Buhot, N., Gomes, E., Milat, M.L., Ponchet, M., Marion, D., Lequeu, J., Delrot, S., Coutos-Thevenot, P., Blein, J.P., 2004. Modulation of the biological activity of a tobacco LTP1 by lipid complexation. Mol. Biol. Cell 15, 5047–5052.

Chakravarty, S., Varadarajan, R., 2000. Elucidation of determinants of protein stability through genome sequence analysis. FEBS Lett. 470, 65–69.

Chan, C.S., Guo, L., Shih, M.C., 2001. Promoter analysis of the nuclear gene encoding the chloroplast glyceraldehyde-3-phosphate dehydrogenase B subunit of *Arabidopsis thaliana*. Plant Mol. Biol. 46, 131–141.

Chen, H., Nelson, R.S., Sherwood, J.L., 1994. Enhanced recovery of transformants of *Agrobacterium tumefaciens* after freeze-thaw transformation and drug selection. Biotechniques 16, 664–668, 670.

Chen, W., Provart, N.J., Glazebrook, J., Katagiri, F., Chang, H.S., Eulgem, T., Mauch, F., Luan, S., Zou, G., Whitham, S.A., Budworth, P.R., Tao, Y., Xie, Z., Chen, X., Lam, S., Kreps, J.A., Harper, J.F., Si-Ammour, A., Mauch-Mani, B., Heinlein, M., Kobayashi, K., Hohn, T., Dangl, J.L., Wang, X., Zhu, T., 2002. Expression profile matrix of Arabidopsis transcription factor genes suggests their putative functions in response to environmental stresses. Plant Cell 14, 559–574.

Compton, L.A., Johnson Jr., W.C., 1986. Analysis of protein circular dichroism spectra for secondary structure using a simple matrix multiplication. Anal. Biochem. 155, 155–167.

Cook, M.E., Graham, L.E., 1998. Structural similarities between surface layers of selected charophycean algae and bryophytes and the cuticles of vascular plants. Int. J. Plant Sci. 159, 780–787.

Das, S., Paul, S., Bag, S.K., Dutta, C., 2006. Analysis of nanoarchaeumequitans genome and proteome composition: indications for hyperthermophilic and parasitic adaptation. BMC Genom. 7, 186.

Davis, S.J., Vierstra, R.D., 1996. Soluble derivatives of green fluorescent protein (GFP) for use in *Arabidopsis thaliana*. Weeds World 3, 43–48.

Debono, A., Yeats, T.H., Rose, J.K., Bird, D., Jetter, R., Kunst, L., Samuels, L., 2009. Arabidopsis LTPG is a glycosylphosphatidylinositol-anchored lipid transfer protein required for export of lipids to the plant surface. Plant Cell 21, 1230–1238.

Douliez, J.P., Pato, C., Rabesona, H., Mollé, D., Marion, D., 2001. Disulfide bond assignment, lipid transfer activity and secondary structure of a 7-kDa plant lipid transfer protein, LTP2. Eur. J. Biochem. 268, 1400–1403.

Dunn, M.A., White, A.J., Vural, S., Hughes, M.A., 1998. Identification of promoter elements in a low-temperature-responsive gene (blt4.9) from barley (*Hordeum vulgare* L.). Plant Mol. Biol. 38, 551–564.

Edqvist, J., Farbos, I., 2002. Characterization of germination-specific lipid transfer proteins from *Euphorbia lagascae*. Planta 215, 41–50.

Edqvist, J., Ronnberg, E., Rosenquist, S., Blomqvist, K., Viitanen, L., Salminen, T.A., Nylund, M., Tuuf, J., Mattjus, P., 2004. Plants express a lipid transfer protein with high similarity to mammalian sterol carrier protein-2. J. Biol. Chem. 279, 53544–53553.

Edstam, M.M., Blomqvist, K., Eklöf, A., Wennergren, U., Edqvist, J., 2013. Coexpression patterns indicate that GPI-anchored non-specific lipid transfer proteins are involved in accumulation of cuticular wax, suberin and sporopollenin. Plant Mol. Biol. 83, 625–649.

Edstam, M.M., Viitanen, L., Salminen, T.A., Edqvist, J., 2011. Evolutionary history of the non-specific lipid transfer proteins. Mol. Plant 4, 947–964.

Eklund, D.M., Edqvist, J., 2003. Localization of non-specific lipid transfer proteins correlate with programmed cell death responses during endosperm degradation in *Euphorbia lagascae* seedlings. Plant Physiol. 132, 1249–1259.

Eklund, D.M., Thelander, M., Landberg, K., Staldal, V., Nilsson, A., Johansson, M., Valsecchi, I., Pederson, E.R., Kowalczyk, M., Ljung, K., Ronne, H., Sundberg, E., 2010. Homologues of the *Arabidopsis thaliana* SHI/STY/LRP1 genes control auxin biosynthesis and affect growth and development in the moss *Physcomitrella patens*. Development 137, 1275–1284.

Fowler, S., Thomashow, M.F., 2002. Arabidopsis transcriptome profiling indicates that multiple regulatory pathways are activated during cold acclimation in addition to the CBF cold response pathway. Plant Cell 14, 1675–1690.

Franke, R., Briesen, I., Wojciechowski, T., Faust, A., Yephremov, A., Nawrath, C., Schreiber, L., 2005. Apoplastic polyesters in Arabidopsis surface tissues-a typical suberin and a particular cutin. Phytochemistry 66, 2643–2658.

Gaier, S., Marsh, J., Oberhuber, C., Rigby, N.M., Lovegrove, A., Alessandri, S., Briza, P., Radauer, C., Zuidmeer, L., van Ree, R., Hemmer, W., Sancho, A.I., Mills, C., Hoffmann-Sommergruber, K., Shewry, P.R., 2008. Purification and structural stability of the peach allergens Pru p 1 and Pru p 3. Mol. Nutr. Food Res. 52, S220–S229.

Gasteiger, E., Hoogland, C., Gattiker, A., Duvaud, S., Wilkins, M.R., Appel, R.D., Bairoch, A., 2005. Protein identification and analysis tools on the ExPASy server. In: Walker, John M. (Ed.), The Proteomics Protocols Handbook. Humana Press, pp. 571–607.

Gincel, E., Simorre, J.P., Caille, A., Marion, D., Ptak, M., Vovelle, F., 1994. Three-dimensional structure in solution of a wheat lipid-transfer protein from multidimensional 1H-NMR data. A new folding for lipid carriers. Eur. J. Biochem. 226, 413–422.

Guerbette, F., Grosbois, M., Jolliot-Croquin, A., Kader, J.C., Zachowski, A., 1999. Comparison of lipid binding and transfer properties of two lipid transfer proteins from plants. Biochemistry 38, 14131–14137.

Guindon, S., Dufayard, J.F., Lefort, V., Anisimova, M., Hordijk, W., Gascuel, O., 2010. New algorithms and methods to estimate maximum-likelihood phylogenies: assessing the performance of PhyML 3.0. Syst. Biol. 59, 307–321.

Guo, C., Ge, X., Ma, H., 2013a. The rice OsDIL gene plays a role in drought tolerance at vegetative and reproductive stages. Plant Mol. Biol. 82, 239–253.

Guo, L., Yang, H., Zhang, X., Yang, S., 2013b. Lipid transfer protein 3 as a target of MYB96 mediates freezing and drought stress in Arabidopsis. J. Exp. Bot 64, 1755–1767.

Hiratsuka, K., Chua, N.H., 1997. Light regulated transcription in higher plants. J. Plant Res. 110, 131–139.

Hoh, F., Pons, J.L., Gautier, M.F., de Lamotte, F., Dumas, C., 2005. Structure of a liganded type 2 non-specific lipid-transfer protein from wheat and the molecular basis of lipid binding. Acta Crystallogr. Sect. D-Biol. Crystallogr. 61, 397–406.

Holm, K., Kallman, T., Gyllenstrand, N., Hedman, H., Lagercrantz, U., 2010. Does the core circadian clock in the moss *Physcomitrella patens* (Bryophyta) comprise a single loop? BMC Plant Biol. 10, 109.

Hu, Y.X., Wang, Y.X., Liu, X.F., Li, J.Y., 2004. Arabidopsis RAV1 is down-regulated by brassinosteroid and may act as a negative regulator during plant development. Cell Res. 14, 8–15.

Hudson, M.E., Quail, P.H., 2003. Identification of promoter motifs involved in the network of phytochrome A-regulated gene expression by combined analysis of genomic sequence and microarray data. Plant Physiol. 133, 1605–1616.

Ikezawa, H., 2002. Glycosylphosphatidylinositol (GPI)-anchored proteins. Biol. Pharm. Bull. 25, 409–417.

Kader, J.C., 1975. Proteins and the intracellular exchange of lipids. I. Stimulation of phospholipid exchange between mitochondria and microsomal fractions by proteins isolated from potato tuber. Biochim. Biophys. Acta 380, 31–44.

Kader, J.C., 1996. Lipid-transfer proteins in plants. Annu. Rev. Plant Physiol. Plant Mol. Biol. 47, 627–654.

Kim, H., Lee, S.B., Kim, H.J., Min, M.K., Hwang, I., Suh, M.C., 2012. Characterization of glycosylphosphatidylinositol-anchored lipid transfer protein 2 (LTPG2) and overlapping function between LTPG/LTPG1 and LTPG2 in cuticular wax export or accumulation in *Arabidopsis thaliana*. Plant Cell Physiol. 53, 1391–1403.

Kim, S.Y., Chung, H.J., Thomas, T.L., 1997. Isolation of a novel class of bZIP transcription factors that interact with ABA-responsive and embryo-specification elements in the Dc3 promoter using a modified yeast one-hybrid system. Plant J. 11, 1237–1251.

Kumar, S., Tsai, C.J., Nussinov, R., 2000. Factors enhancing protein thermostability. Protein Eng. 13, 179–191.

Lakhan, S.E., Sabharanjak, S., De, A., 2009. Endocytosis of glycosylphosphatidylinositol-anchored proteins. J. Biomed. Sci. 16, 93.

Lascombe, M.B., Bakan, B., Buhot, N., Marion, D., Blein, J.P., Larue, V., Lamb, C., Prange, T., 2008. The structure of “defective in induced resistance” protein of *Arabidopsis thaliana*, DIR1, reveals a new type of lipid transfer protein. Prot. Sci. 17, 1522–1530.

Le, S.Q., Gascuel, O., 2008. An improved general amino acid replacement matrix. Mol. Biol. Evol. 25, 1307–1320.

Lee, J.Y., Min, K., Cha, H., Shin, D.H., Hwang, K.Y., Suh, S.W., 1998. Rice non-specific lipid transfer protein: the 1.6 A crystal structure in the unliganded state reveals a small hydrophobic cavity. J. Mol. Biol. 276, 437–448.

Lee, S.B., Go, Y.S., Bae, H.J., Park, J.H., Cho, S.H., Cho, H.J., Lee, D.S., Park, O.K., Hwang, I., Suh, M., 2009. Disruption of glycosylphosphatidylinositol-anchored lipid transfer protein gene altered cuticular lipid composition, increased plastoglobules, and enhanced susceptibility to infection by the fungal pathogen *Alternaria brassicicola*. Plant Physiol. 150, 42–54.

Lehtonen, J.V., Still, D.J., Rantanen, V.V., Ekholm, J., Bjorklund, D., Iftikhar, Z., Huhtala, M., Repo, S., Jussila, A., Jaakkola, J., Pentikainen, O., Nyronen, T., Salminen, T., Gyllenberg, M., Johnson, M.S., 2004. BODIL: a molecular modeling environment for structure-function analysis and drug design. J. Comput.-Aided Mol. Des. 18, 401–419.

Lerche, M.H., Poulsen, F.M., 1998. Solution structure of barley lipid transfer protein complexed with palmitate. Two different binding modes of palmitate in the homologous maize and barley nonspecific lipid transfer proteins. Prot. Sci. 7, 2490–2498.

Lin, K.F., Liu, Y.N., Hsu, S.T., Samuel, D., Cheng, C.S., Bonvin, A.M., Lyu, P.C., 2005. Characterization and structural analyses of nonspecific lipid transfer protein 1 from mung bean. Biochemistry 44, 5703–5712.
Lindorff-Larsen, K., Winther, J.R., 2001. Surprisingly high stability of barley lipid transfer protein, LTP1, towards denaturant, heat and proteases. FEBS Lett. 488, 145–148.
Livak, K.J., Schmittgen, T.D., 2001. Analysis of relative gene expression data using real-time quantitative PCR and the $2^{-\Delta\Delta CT}$ method. Methods 25, 402–408.
Lobley, A., Whitmore, L., Wallace, B.A., 2002. DICHROWEB: an interactive website for the analysis of protein secondary structure from circular dichroism spectra. Bioinformatics 18, 211–212.
Maldonado, A.M., Doerner, P., Dixon, R.A., Lamb, C.J., Cameron, R.K., 2002. A putative lipid transfer protein involved in systemic resistance signalling in Arabidopsis. Nature 419, 399–403.
Manavalan, P., Johnson Jr., W.C., 1987. Variable selection method improves the prediction of protein secondary structure from circular dichroism spectra. Anal. Biochem. 167, 76–85.
Müller, A., Kloppel, C., Smith-Valentine, M., Van Houten, J., Simon, M., 2012. Selective and programmed cleavage of GPI-anchored proteins from the surface membrane by phospholipase C. Biochim. Biophys. Acta 1818, 117–124.
Neinhuis, C., Jetter, R., 1995. Ultrastructure and chemistry of epicuticular wax crystals in Polytrichales sporophytes. J. Bryol. 18, 399–406.
Nishiyama, T., Hiwatashi, Y., Sakakibara, I., Kato, M., Hasebe, M., 2000. Tagged mutagenesis and gene-trap in the moss, *Physcomitrella patens* by shuttle mutagenesis. DNA Res. 7, 9–17.
Pack, S.P., Yoo, Y.J., 2004. Protein thermostability: structure-based difference of amino acid between thermophilic and mesophilic proteins. J. Biotechnol. 111, 269–277.
Park, C.J., Shin, R., Park, J.M., Lee, G.J., You, J.S., Paek, K.H., 2002. Induction of pepper cDNA encoding a lipid transfer protein during the resistance response to tobacco mosaic virus. Plant Mol. Biol. 48, 243–254.
Park, S.Y., Lord, E.M., 2003. Expression studies of SCA in lily and confirmation of its role in pollen tube adhesion. Plant Mol. Biol. 51, 183–189.
Pollard, M., Beisson, F., Li, Y., Ohlrogge, J.B., 2008. Building lipid barriers: biosynthesis of cutin and suberin. Trends Plant Sci. 13, 236–246.
Pons, J.L., de Lamotte, F., Gautier, M.F., Delsuc, M.A., 2003. Refined solution structure of a liganded type 2 wheat nonspecific lipid transfer protein. J. Biol. Chem. 278, 14249–14256.
Razvi, A., Scholtz, J.M., 2006. Lessons in stability from thermophilic proteins. Prot. Sci. 15, 1569–1578.
Sali, A., Blundell, T.L., 1993. Comparative protein modelling by satisfaction of spatial restraints. J. Mol. Biol. 234, 779–815.
Samuel, D., Liu, Y.J., Cheng, C.S., Lyu, P.C., 2002. Solution structure of plant nonspecific lipid transfer protein-2 from rice (*Oryza sativa*). J. Biol. Chem. 277, 35267–35273.
Sancho, A.I., Rigby, N.M., Zuidmeer, L., Asero, R., Mistrello, G., Amato, S., González-Mancebo, E., Fernández-Rivas, M., van Ree, R., Mills, E.N., 2005. The effect of thermal processing on the IgE reactivity of the non-specific lipid transfer protein from apple, Mal d 3. Allergy 60, 1262–1268.
Sawano, Y., Hatano, K., Miyakawa, T., Komagata, H., Miyauchi, Y., Yamazaki, H., Tanokura, M., 2008. Proteinase inhibitor from ginkgo seeds is a member of the plant nonspecific lipid transfer protein gene family. Plant Physiol. 146, 1909–1919.
Schlenk, H., Gellerman, J.L., 1965. Arachidonic, 5, 11, 14, 17-eicosatetraenoic and related acids in plants-identification of unsaturated fatty acids. J. Am. Oil Chem. Soc. 42, 504–511.
Shin, D.H., Lee, J.Y., Hwang, K.Y., Kim, K.K., Suh, S.W., 1995. High-resolution crystal structure of the non-specific lipid-transfer protein from maize seedlings. Structure 3, 189–199.
Sigrist, C.J., Cerutti, L., de Castro, E., Langendijk-Genevaux, P.S., Bulliard, V., Bairoch, A., Hulo, N., 2010. PROSITE, a protein domain database for functional characterization and annotation. Nucleic Acids Res. 38, D161–D166.
Smith, L.J., Roby, Y., Allison, J.R., van Gunsteren, W.F., 2013. Molecular dynamics simulations of barley and maize lipid transfer proteins show different ligand binding preferences in agreement with experimental data. Biochemistry 52, 5029–5038.
Sparkes, I.A., Runions, J., Kearns, A., Hawes, C., 2006. Rapid, transient expression of fluorescent fusion proteins in tobacco plants and generation of stably transformed plants. Nat. Protoc. 1, 2019–2025.
Sreerama, N., Woody, R.W., 2000. Estimation of protein secondary structure from CD spectra: comparison of CONTIN, SELCON and CDSSTR methods with an expanded reference set. Anal. Biochem. 287, 252–260.
Sterk, P., Booij, H., Schellekens, G.A., Van Kammen, A., De Vries, S.C., 1991. Cell-specific expression of the carrot EP2 lipid transfer protein gene. Plant Cell 3, 907–921.
Thoma, S., Hecht, U., Kippers, A., Botella, J., De Vries, S., Somerville, C., 1994. Tissue-specific expression of a gene encoding a cell wall-localized lipid transfer protein from Arabidopsis. Plant Physiol. 105, 35–45.
Thompson, J.D., Higgins, D.G., Gibson, T.J., 1994. CLUSTAL W: improving the sensitivity of progressive multiple sequence alignment through sequence weighting, position-specific gap penalties and weight matrix choice. Nucleic Acids Res. 22, 4673–4680.
Tomassen, M.M., Barrett, D.M., van der Valk, H.C., Woltering, E.J., 2007. Isolation and characterization of a tomato non-specific lipid transfer protein involved in polygalacturonase-mediated pectin degradation. J. Exp. Bot. 58, 1151–1160.
Whitmore, L., Wallace, B.A., 2004. DICHROWEB: an online server for protein secondary structure analyses from circular dichroism spectroscopic data. Nucleic Acids Res. 32, W668–W673.
Whitmore, L., Wallace, B.A., 2008. Protein secondary structure analyses from circular dichroism spectroscopy: methods and reference databases. Biopolymers 89, 392–400.
Willard, L., Ranjan, A., Zhang, H., Monzavi, H., Boyko, R.F., Sykes, B.D., Wishart, D.S., 2003. VADAR: a web server for quantitative evaluation of protein structure quality. Nucleic Acids Res. 31, 3316–3319.
Woo, H.R., Kim, J.H., Kim, J., Kim, J., Lee, U., Song, I.J., Kim, J.H., Lee, H.Y., Nam, H.G., Lim, P.O., 2010. The RAV1 transcription factor positively regulates leaf senescence in Arabidopsis. J. Exp. Bot. 61, 3947–3957.
Xu, Z., Liu, Y., Yang, Y., Jiang, W., Arnold, E., Ding, J., 2003. Crystal structure of D-hydantoinase from *Burkholderia pickettii* at a resolution of 2.7 Angstroms: insights into the molecular basis of enzyme thermostability. J. Bact. 185, 4038–4049.
Yuan, J.S., Reed, A., Chen, F., Stewart Jr., C.N., 2006. Statistical analysis of real-time PCR data. BMC Bioinform. 7, 85.
Zachowski, A., Guerbette, F., Grosbois, M., Jolliot-Croquin, A., Kader, J.C., 1998. Characterisation of acyl binding by a plant lipid-transfer protein. Eur. J. Biochem. 257, 443–448.
Zhou, X.X., Wang, Y.B., Pan, Y.J., Li, W.F., 2008. Differences in amino acids composition and coupling patterns between mesophilic and thermophilic proteins. Amino Acids 34, 25–33.